MANY-BODY IS QUANTUM DOTS

by

PATRICK MERLOT

THESIS
for the degree of
MASTER OF SCIENCE

(Solid State and Computational Physics)

Faculty of Mathematics and Natural Sciences
Department of Physics
University of Oslo

August 2009

Contents

Contents

Chapter 1

Introduction

1.0.1 [Subject and Definitions]

Following their recent successes in describing and predicting properties of materials, electronic structure calculations using numerical computation have become increasingly important in the fields of physics and chemistry over the past decade, especially with the development of supercomputers. From the basic constituants of a system of particles and their interactions, a computational approach enables to derive the electronic structure and the properties of the system.

A system of particles that is currently considered with attention is the quantum dot: it is an artificial system consisting of several interacting electrons confined to small regions between layers of semiconductors. The whole system can be seen as a nanoscopic box of semiconductor with exceptional electrical and optical properties. Applications based on quantum dots are developped in numerous fields of medicine and modern electronics.

1.0.2 [Overview + Motivation + contribution]

This thesis describes a computional study of a quantum dot in two dimensions. It presents the methods used in numerical simulations and some many-body techniques with various levels of sophistication: Hartree-Fock method, perturbation theory, variational Monte-Carlo and large scale diagonalisation (e.g. full configuration interaction) techniques. It focuses on the restricted Hartree-Fock method, one of the fastest and cheapest techniques but also one of the less accurate. The aim of the study is to assess the pertinence of this method to study quantum dots in two-dimensions confined by a spherical potential and squeezed by an external magnetic field. Results from Hartree-Fock can be used alone, or used as inputs to other ab-initio methods like

perturbation theory (PT), variational Monte-Carlo (VMC) or full configuration interaction (FCI). Similar Hartree-Fock studies were performed by Johnson and Reina in 1992 [1] and Pfannkuche in 1993 [2]. In addition here the results from Hartree-Fock are compared to the results obtained with other techniques developped by my colleagues: Rune Albrigtsen with variational Monte-Carlo [3] and Simen Kvaal with configuration interaction method with and without effective interaction [4].

1.0.3 [My contribution, guide to the reader]

what I have done? be able to discuss my contribution to the problem compared to what's existing

paper on the limit of Hartree-Fock

short description of the results:

– A Hartree-Fock simulator has been developped in 2D.

– what are the limitations of HF according to the strength of the confinement wrt other methods?

  – accuracy wrt to the size of the system?

  – accuracy wrt to strength of the confinement?

  – simulation duration (compare the limits of each method for a given system, and compare the size of the biggest system achievable by each method-> other method like DFT might be of interest to study huge system in a reasonnable amount of time)?

  – Are HF results accurate enough for the confinement (B field) in use today in laboratories for confining electrons in a quantum dot?

  – HOW fast HF converges wrt other ab initio methods? It is possible to explicitely give the convergence rate?

– what are the improvements when using the HF basis set as input of VMC or CI?

1.0.4 [structure of the thesis]

This thesis is organized as follows. Chapter 2 briefly discusses the story of quantum dots and legitimates the quest for more accurate models and their numerical simulations. In chapter 3 phenomenological aspects and properties of the QD are described as well as some techniques in use today for building and manipulating those artificial systems.

Chapter 4 reviews some models of QD leading to the theoretical approximation used in this thesis. Some particular cases solvable analytically are developped and used as references when checking the stability and accuracy of the simulator. When it comes to the treatment of the QD model for numerical simulation, chapter 5 introduces the Hartree-Fock theory as one possible many-body technique and the resulting iterative procedure is worked out for different possible implementations.

Chapter 6 describes the computational implementation of the Hartree-Fock techniques applied to the QD model. Results are provided for closed shell systems, compared to other *ab initio* many-body techniques and a numerical analysis provides information on the convergence behaviour of Hartree-Fock.

Concluding remarks and suggestions for futur work are given in chapter 8 while most calculations are done in the appendix to minimize the number of equations inside the chapters.

Chapter 2

History and Motivations

In our current understanding of nanotechnology, quantum dots reign supreme as the most functional and reproducible nanostructures available to researchers. Common shapes include pyramids, cylinders, lens shapes, and spheres. Different synthesis routes create different kinds of quantum dots. They are very small by nature, the smallest objects that we can synthesize on the nanoscale. From this fact, they are assimilated to dots, though one quantum dot can be made out of roughly a million atoms. All the atoms pool their electrons to "sing with one voice", that is, the electrons are shared and coordinated as if there is only one atomic nuclei attraction at the centre. That property enables numerous revolutionary schemes for electronic devices and quantum dots are often referred to as artificial atoms.

The total diameter of a quantum dot varies between 2-10 nm depending on its application, corresponding to 10-50 atoms in diameter and a total of $100 - 100,000$ atoms within the quantum dot volume [5] with an equivalent number of electrons. Virtually all electrons are tightly bound to the nuclei of those atoms, however the number of "free electron" in the dot can be very small: between one or a few hundred [6]. The reason 'quantum' prefixes the name is because the dots exhibit quantum confinement properties in all three dimensions. This means that electrons within the dot can't freely move around in any direction leading to quantization as we will show in 3. The only thing that behaves like this in nature is the atom. Unlike an atom, a quantum dot is tunable and at least ten times bigger. This has a lot of important consequences for researchers. First of all they exhibit quantized energy levels like an atom. For a given energy of excitation, for instance, a quantum dot will only emit specific spectra of light. Quantum theory predicts that with decreasing their diameters, there will be a corresponding increase in frequency (e.g. in energy) of the emitted light.

This element of control over quantum dots' emission properties has huge

implications for both electronic devices and medical applications. Due to their excellent confinement properties not seen in nanowires or quantum wells, quantum dots are extremely efficient at emitting light. They have been the source of some of the world's most powerful lasers produced to date, though the practicality of a quantum dot laser is still being improved. In medical studies, quantum dots are already in practice as tags that can be inserted into patients. These tags can be seen under most medical scanning technologies and can help pinpoint biological processes as they occur.

2.1 History of Quantum Dots

In the late 50's began the first studies of artificial quantum systems, mostly theoretical due to the lack of funds. In the 60's, epitaxial depositions was developed and with it, the possibility to build ultra-clean composite layers of semiconductor material sandwiched between two other layers of another semiconductor. The first optical properties were discovered and the two-dimensional character of the sample has been observed. At the beginning of the 80's, rapid progress in technology were made with accurate lithography technics (the first quasi one-dimensional quantum wire was done with these progress) [7].

Colloïdal quantum dots were discovered in 1981, during the development of materials for the photo-cleavage of water. Bulk cadmium sulfide (CdS) is known to be an ideal electrode material; however it experiences photocorrosion upon irradiation. It was believed that colloidal particles of cadmium sulfide, coated with a protective agent (i.e. RuO_2), would be more resistant to corrosion. Therefore, a synthesis method was developed to produce colloidal CdS through aqueous precipitation. The resulting particles displayed unique properties not found in the bulk, including fluorescent emission. These properties were determined to be the result of quantum size effects [8], and were found to be tunable by altering the size of the particle [9]. This provided a method for selecting excitation and emission wavelengths and particle band gaps.

In the middle of the 80's, the first quantum dot was developed based on etching technique [Reed et al.;1986]. As a consequence, a complete quantization of the electron free motion was possible. At the end of the 80's and in the 90's, the methods evolved: lithography and etching are still in use, but electron or ion-lithography have replaced light-lithography and so increased precision [7].

Lent predicted in 1993 the need for building quantum cellular automata

(QCA) cells of 2 nm in order to work at room temperature, where quantum cellular automata refers to any models of quantum computation.

"Ultimately, temperature effects are the principal problem to be overcome in physically realizing the QCA computing paradigm. The critical energy is the energy difference between the ground state and the first excited state of the array. If this is sufficiently large compared with $k_B T$, the system will be reliably in the ground state after a characteristic relaxation time. Fortunately, this energy difference increases quadratically as the cell dimensions shrink. If the cell size could be made a few Ångstroms, the energy differences would be comparable to atomic energy levels (i.e. several electron-Volts!)". "As technology advances to smaller and smaller dimensions on the few-nanometer scale, the temperature of operation will be allowed to increase. Perhaps our envisioned QCA will find its first room temperature implementation in molecular electronics." [10]

Interest in the use of quantum dots in biomedicine began in 1998. Coupling the quantum dots directly to biorecognition molecules (e.g. antibodies, proteins), the particles could be targeted to particular parts of the cell, producing a fluorescent indicator [11,12].

Early this year (Jan. 2009), the four-quantum dot cell dreamed by Lent has now been achieved with the fabrication and control of a 1 nm-scale assembly of four coupled silicon dangling bond (DB). Indeed single atom quantum dots created by researchers in Canada make possible a new level of control over individual electrons, a development that suddenly brings quantum dot-based devices within reach [13]. **Composed of a single atom of silicon and measuring less than one nanometre in diameter, these are the smallest quantum dots ever created**. Until now, quantum dots have been useable only at impractically low temperatures, but the new atom-sized quantum dots perform at room temperature. And because they operate at room temperature and exist on the familiar silicon crystals used in today's computers, researchers expect these single atom quantum dots to transform theoretical plans into real devices. Figure (2.1) shows how atom-sized QD can be manipulated at room temperature. The single atom quantum dots have also demonstrated another advantage: significant control over individual electrons by using very little energy. This low energy control is seen as the key to quantum dot application in entirely new forms of silicon-based electronic devices, such as ultra low power computers.

Figure 2.1: Two coupled atomic quantum dots are shown in this room temperature scanning tunneling microscopy image. In the top frame the dots share one electron. The electron moves freely between the dots just like an electron in a chemical bond within a molecule. The lower frame demonstrates control over that single electron and the potential to do computations in a new way. The electric field from the control charge pushes the electron to prefer staying on only one of the quantum dots. (Image courtesy of University of Alberta/Prof. Robert A. Wolkow)
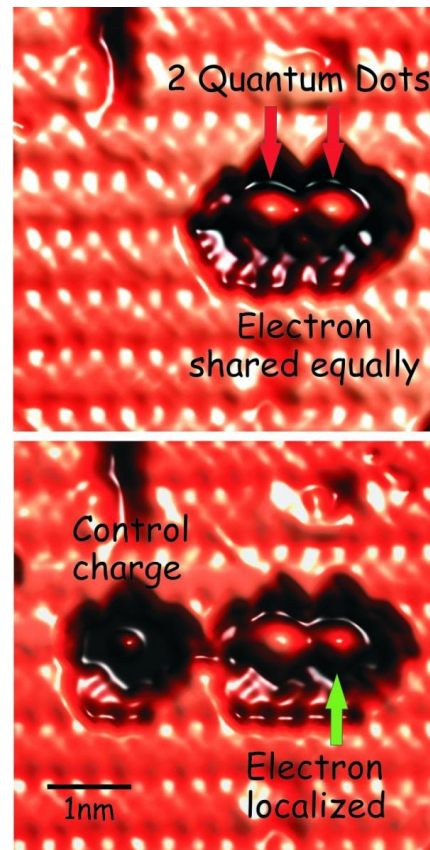
2.2 Some applications of QD

Exceptional electrical and optical properties make quantum dots **attractive components for integration into electronic devices**. One significant asset of quantum dots over traditional optoelectronic materials is that they exist in the solid state. Solids tend to be more compact, easly cooled, and allow for direct charge injection. Additionally, quantum dots can interconvert light and electricity in a tunable manner dependant on crystal size, allowing for easy wavelength selection. This is a significant improvement over silicon-based materials, which require modification of their chemical composition (i.e. doping) to alter optical properties [14]. Thus researchers have experimented with quantum dots in lasers, LEDS, photovoltaics and also for new generations of transistors, prototypes of spin devices, logic gates with quantum computers as a final aim. Most of these applications are still in early development; however the benefits of quantum dot components are evident, soon leading to a complete revolution of the way of building electronic components at atomic scale.

Also one of the fastest moving and most exciting interfaces of nanotechnology is the use of (colloïdal) **quantum dots in biology**. Again their unique optical properties make them appealing as *in vitro* and *in vivo* fluorophores in a variety of biological investigations, in which traditional fluorescent labels based on organic molecules fall short of providing long-term stability and simultaneous detection of multiple signals [15]. The ability to make quantum dots water soluble and target them to specific biomolecules has led to promising applications in cellular labelling, thus improving diagnostic methods (ex. tracking cancer cells *in vivo* during metastasis [16, 17, 18]) and in developing better drug delivery systems to improve disease therapy [19]. It is even currently studied as neuroelectronic interface for converting optical energy into electrical signal responding to the need for prosthetic devices that can repair or replace nerve function [20]. However there are still many open questions about the toxicity of inorganic QD. The size and charge of most nanoparticles preclude their efficient clearance from the body as intact nanoparticles. Without such clearance or their biodegradation into biologically benign components, toxicity is potentially amplified and radiological imaging is hindered. Some neutral organic coatings prevents adsoption of serum proteins (which otherwise increased the total diameter by $> 15nm$ and prevent renal clearance). A final hydrodynamic diameter $< 5.5nm$ resulted in rapid and efficient urinary excretion and elimination of quantum dots from the body [21].

These achievements, even in their premises, have laid the **foundations for theoretical investigations** to enable advances in the understanding

of the fundamental structure, stability and aqueous assembly of nanoparticle architectures. A physical systems consisting of between $10s - 1000s$ of atoms is already too complex to be studied otherwise than using numerical methods for a reliable description. The concept of artificial atom can even be generalized to artificial molecules.

Moreover QDs appears as good tools for studying atomic spectra of manybody systems on a theoretical point of view using computational techniques. Thanks to the possibility to build our own artificial atoms without considering the complexity of the nucleus, it becomes simpler to confront numerical and experimental results.

2.3   Clarifications about computational studies

The usefulness of numerical simulation is more and more recognized and today it is used in many domains of research and development: mechanics, fluid mechanics, solid state physics, astrophysics, nuclear physics, climatology, quantum mechanics, biology, chemistry... More than being limited to scientific subjects numerical simulation is also used in human sciences (demography, sociology) as well as in finance or economy.

In physics, beside the importance for our basic understanding of quantal systems, the capability to develop and study stable numerical quantum mechanical systems with many degrees of freedom is of great importance, as analytic solutions are rare or impossible to obtain.

Some definitions:

A numerical simulation reproduces the fundamental behaviour of a complex system in order to study its properties and predict its evolution. It is based on the implementation of theoretical models, ie it is an adaptation of mathematical models to numerical tools. Data mining and virtual reality are different from numerical simulation and should not be mistaken with it.

A numerical simulation is performed in several steps:

The model   describes the system analysed by listing its essential parameters and by writing the physical laws that rule its behaviour (and link the parameters) as mathematical equations.

The simulation   itself is the translation of the equations into computer language, associated with the discretization of the physical domain to make it finite (select a time step, a finite number of points, an acceptable level of accuracy, etc)

Computational techniques   The resolution of the equations leads to the determination of the numerical values of all the parameters of the system in every points, ie the state of the system is known. Various computational techniques can be used to solve the equations, they can be grouped into two main approaches: the deterministic and the statistical (or probabilistic) methods.

In the first approach, an algorithm will solve predictably the equations. For example the object (or the domain) is discretized and the parameters of each element are linked to its neighbours through algebraic equations. It is up to the computer to solve the system that links all the equations. A deterministic method will always produce the same output when given the same input, and the underlying machine will always go through the same sequence of states (which is why it is called "deterministic"). The Hartree-Fock method used in this thesis belongs to this category as well as the Finite element method or the large scale diagonalisation.

The second approach, which groups the âĂIJMonte-CarloâĂİ methods, is particularly suited to phenomena characterized by a sequence of steps in which each element of the object can be affected by different âĂIJa prioriâĂİ possible events. From step to step, the evolution of the sample will be determined through a random draw (the name of the method comes from this idea)

Validation of the results: the theoretical model and its translation into computer programming must be validated by comparing with experimental data, or by testing a very simple case for which an analytical solution can be found.

Numerical simulations   once validated, can explore more cases or unused configurations that were not tested by experiments, sometimes predicting unexpected behaviours, leading to a greater knowledge of the physical behaviour of the system. Therefore numerical simulation is the third form of study of phenomena, after theory and experiment.

Chapter 3

Physics of Quantum Dots: the artificial atoms

A quantum dot is a semiconductor whose charge-carries are confined in all three spatial dimension, so much confined that quantum effects become visible in many ways: fluorescent effect, quantized conductance, quantized energy spectrum, etc.

So the exceptional properties of quantum dots rely on the fact that one can manipulate the electrons present in it and quite easily observe the change it produces. Whereas the most sophisticated flash memory devices use thousands of electrons to store a bit of information, imagine what you could do with new devices like quantum dots while manipulating a single electron. This opens the door for ultra-low power electronics, further miniaturization and new opto-electronic devices as briefly described in section 2.2. with a lot of amazing applications.

The physics behind it involves the (electronic) structure of the material (here mainly semiconductors) and some basic quantum mechanical effects such as size quantization, quantum tunneling or Coulomb blockade.

In this chapter, some basic quantum mechanical effects leading to the properties of quantum dots are reviewed. First we discuss the requirements for quantum confinement in a semiconductor, as well as the changes in the energy band structure. These are related to the resulting electrical and optical phenomena and constrasted with the properties of bulk materials.

3.1 Size quantization

Before applying quantum theory to quantum dots, let's review some basics of quantum mechanics and particularly how quantization arises and why is it not always noticeable in our everyday life.

The particle in a box Let's consider the well-known example of a particle in a one-dimensional box trapped by an infinite (potential) barrier (see figure 3.1a). The potential $V(x)$ is given below:

$$V(x) = 0, \qquad for\ 0 < x < a$$
$$V(x) = \infty, \qquad for\ x \leq 0, x \geq a \qquad (3.1)$$

How these boundaries can affect the particle? Remember the wave-particle duality and look at the time-independent Schrödinger equation for this system:

$$\frac{d^2\Psi(x)}{dx^2} = \frac{2m}{\hbar^2}\left[V(x) - E\right]\Psi(x) \qquad (3.2)$$

Solutions of the Schrödinger equation, due to boundaries of the box $\Psi(0) = \Psi(a) = 0$ have to fullfill those conditions:

$$\Psi(x) = Asin(kx) + Bcos(kx)$$
$$\Psi(0) = 0 + B = 0 \qquad (3.3)$$
$$\Psi(a) = Asin(ka) = 0$$

This can only be satisfied by $B = 0$ and if either $A = 0$ or if $ka = n\pi$. Setting $A = 0$ would mean that the wave function is always zero, which is unacceptable, we conclude that:

$$\Psi_n(x) = Asin(\frac{n\pi x}{a}), \qquad for\ n = 1, 2, 3, 4, \ldots \qquad (3.4)$$

The constant A can be determined by normalization, by saying that $\Psi_n(x)^*\Psi_n(x)dx$ represents the probability of finding the particle in the interval of width dx centered on x. Because the probability of finding the particle somewhere in the entire interval $[0, a]$ is one,

$$\int_0^a \Psi_n(x)^*\Psi_n(x) = 1$$

so that we obtain the normalized eigenfunctions also plotted in figure 3.1b

$$\Psi_n(x) = \sqrt{\frac{2}{a}}\,sin\left(\frac{n\pi x}{a}\right) \qquad (3.5)$$

(a) The potential

(b) First eigenfunctions

(c) Probability densities
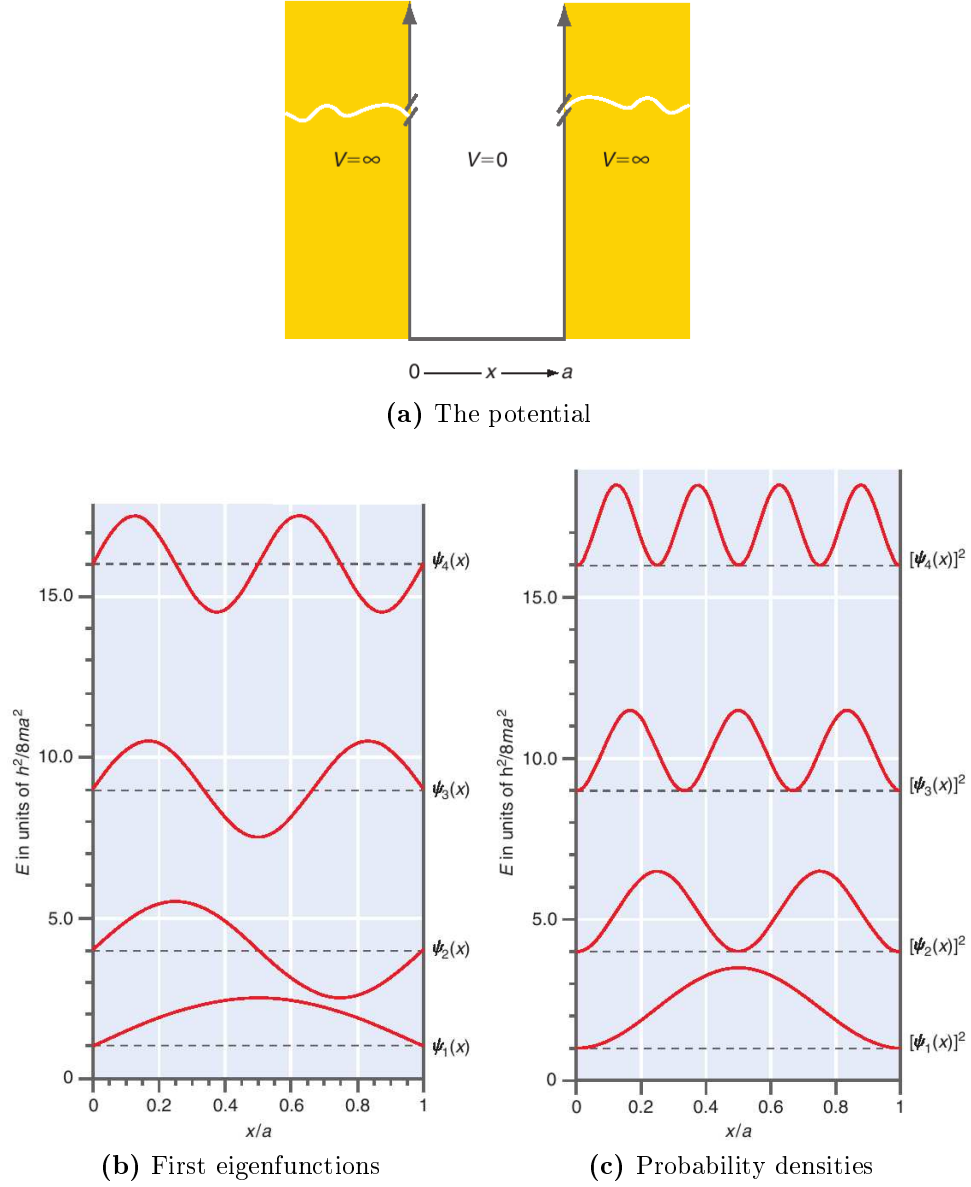
Figure 3.1: (a) The potential described by equation (3.1). Because the particle is confined to the range $0 \le x \le a$, we say that it is confined to a one-dimensional box.
(b) The first few eigenfunctions for the particle in a box are shown together with the corresponding energy eigenvalues. The energy scale is shown on the right with the zero for each level indicated by the dashed line.
(c) The square of the magnitude of the wavefunction, or probability density, is shown as a function of distance together with the corresponding energy eigenvalues. The energy scale is shown on the left. The square of the wave function amplitude is shown on the right with the zero for each level indicated by the dashed line.

Now that we have the eigenfunctions, we can re-introduce them into the Schrödinger equation to find the eigenvalues (i.e. eigen-energies of the system):

$$E_n\Psi_n(x) = -\frac{\hbar^2}{2m}\frac{d^2\Psi_n(x)}{dx^2} \tag{3.6}$$

$$= \frac{\hbar^2}{2m}\left(\frac{n\pi}{a}\right)^2\sqrt{\frac{2}{a}}\,sin\left(\frac{n\pi x}{a}\right) \tag{3.7}$$

Leading to the following expression for the eigenvalues, which are also the possible energies of the system:

$$E_n = \frac{\hbar^2}{2m}\left(\frac{n\pi}{a}\right)^2 = \frac{\hbar^2 n^2}{8ma^2}, \qquad for\ n = 1, 2, 3, \dots \tag{3.8}$$

Compared to a free particle, we see that the energy for a particle in a box is quantized and the integer n is a quantum number. Another important result of the calculation is that the lowest energy allowed is greater than zero. So quantization is just a result of the confinement of the particle. By considering $a \to \infty$, the confinement condition is removed and the discrete energy spectrum becomes continous in this limit. More generally, it means that any particle trapped with some boundaries will experience quantization effect, such as the particle trapped in the dots.

One way to see quantization effects is to look for observables. The total energy is one example of an observable that can be calculated once the eigenfunctions of the time-independent Schrödinger equation are known. Another observable that comes directly from solving this equation is the quantum mechanical analogue of position. Indeed the probability of finding the particle in any interval of width dx in the one-dimensional box is given by $\Psi_n(x)^*\Psi_n(x)dx$. The probability density $\Psi_n(x)^*\Psi_n(x)$ at a given point is shown in figure 3.1b.

Observation of size quantization depending on temperature But how is it possible to observe such quantization effect at our scale? Let's consider the particle to be an electron trapped in a box. The answer will come from the very small constant we have from the Schrödinger equation: the reduced Planck constant $\hbar = h/\pi = 1.05 \times 10^{-34}$ *J.s* $(kg.m^2.s^{-1})$ and the mass of the electron $m = 9.11 \times 10^{-16}$ *kg*. Now the energy to be noticeable should be greater than the thermal energy which is in the order of magnitude of k_BT where $k_B = 1.38 \times 10^{-34}$ *J.K*$^{-1}$ is the Boltzmann constant and T the temperature, otherwise thermal fluctuations will disturb the motion of electrons and will smear out the quantization effects.

At room temperature (i.e. 20℃ $\simeq 293K$), $k_B T \simeq 4.045 \times 10^{-21}$ J. The gap between the first two energy levels should be greater than this value:

$$\Delta E = E_2 - E_1 = \frac{3\hbar^2}{8ma^2} = \frac{4.54 \times 10^{-54}}{a^2} \gtrsim k_B T \qquad (3.9)$$
$$\Rightarrow a \lesssim 1.06 \times 10^{-11} m = 0.0106 \ nm$$

At dilution refrigerator temperatures (i.e. $\sim 100 \ mK$), $k_B T \simeq 1.380 \times 10^{-35}$ J. The gap between the first two energy levels should be greater than this value:

$$\Delta E = E_2 - E_1 = \frac{3\hbar^2}{8ma^2} = \frac{4.54 \times 10^{-54}}{a^2} \gtrsim k_B T \qquad (3.10)$$
$$\Rightarrow a \lesssim 5.734 \times 10^{-10} m = 0.573 \ nm$$

We notice here that it is impossible to observe quantum effect with a such a "free electron" at room temperature, since the box should be roughly the size of an atom, but it could be done at very low temperature.

But now, how is it possible to observe quantization effects in quantum dots, meaning for one or several electrons confined in a semiconductor? We have seen that we actually can not create a dot size at room temperature sufficiently small, but some constants change here when considering the type of material.We will see in the following section that the mass of the charge carries can vary upon the type of material.

3.2   Quantum dots made of semiconductors

A semiconductor is a material that has a resistivity value between that of a conductor and an insulator. The conductivity of a semiconductor material can be varied under an external electrical field.

Most semiconductors on the market are made of silicon (Si). Dozens of other materials are used, including germanium (Ge), gallium arsenide (GaAs). Devices made from semiconductor materials are the foundation of modern electronics, including radio, computers, telephones, and many other devices. Semiconductor devices include the transistor, solar cells, many kinds of diodes including the light-emitting diode, the silicon controlled rectifier, and digital and analog integrated circuits. Solar photovoltaic panels are large semiconductor devices that directly convert light energy into electrical energy.
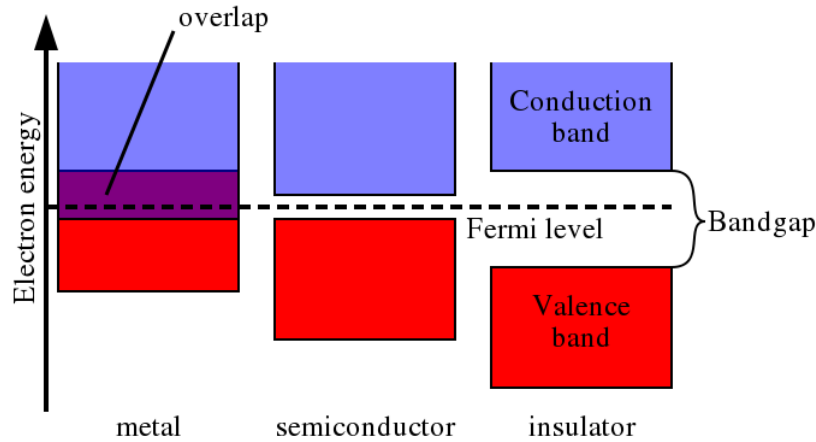
Figure 3.2: Simplfied diagram of the electronic band structure of metals, semiconductors and insulators. (Image courtesy of P. Kuiper)

Energy bands in semiconductors In a metallic conductor, current is carried by the flow of electrons. In semiconductors, current can be carried either by the flow of electrons or by the flow of positively-charged "holes" in the electron structure of the material. Like in other solids and as shown in the previous section 3.1, the electrons in semiconductors can have energies only within certain **energy bands**; between the energy of the **ground state**, corresponding to electrons tightly bound to the atomic nuclei of the material, and the free electron energy, which is the energy required for an electron to escape entirely from the material. The energy bands each correspond to a large number of discrete quantum states of the electrons, and most of the states with low energy (closer to the nucleus) are full, up to a particular band called the **valence band**. Semiconductors and insulators are distinguished from metals because the valence band in the semiconductor materials is very nearly full under usual operating conditions, thus causing more electrons to be available in the **conduction band**, which is the band immediately above the valence band as shown in figure 3.2. The ease with which electrons in a semiconductor can be excited from the valence band to the conduction band depends on the band gap between the bands, and it is the size of this energy bandgap that serves as an arbitrary dividing line between semiconductors and insulators.

In the picture of delocalized states, for example in one dimension that is in a wire, for every energy there is a state with electrons flowing in one direction and one state for the electrons flowing in the other. For a net current to flow some more states for one direction than for the other direction have

to be occupied and for this energy is needed. For a metal this can be a very small energy. In the semiconductor the next higher states lie above the band gap. However, as the temperature of a semiconductor rises above absolute zero, there is more energy in the semiconductor to spend on lattice vibration and on lifting some electrons into an energy states of the conduction band. The current-carrying electrons in the conduction band are known as "**free electrons**", although they are often simply called "electrons" if context allows this usage to be clear.

Electrons excited to the conduction band also leave behind electron holes, or unoccupied states in the valence band. Both the conduction band electrons and the valence band holes (**excitons**) contribute to electrical conductivity. The holes themselves don't actually move, but a neighboring electron can move to fill the hole, leaving a hole at the place it has just come from, and in this way the holes appear to move, and the holes behave as if they were actual positively charged particles.

One covalent bond between neighboring atoms in the solid is ten times stronger than the binding of the single electron to the atom, so freeing the electron does not imply destruction of the crystal structure.

In semiconductors, the dielectric constant is generally large, and as a result, screening tends to reduce the Coulomb interaction between electrons and holes. The result is a Mott-Wannier exciton, which has a radius much larger than the lattice spacing. As a result, the effect of the lattice potential can be incorporated into the **effective masses** of the electron and hole (see table 3.1 for typical values), and because of the lower masses and the screened Coulomb interaction, the binding energy is usually much less than a hydrogen atom, typically on the order of 0.1 eV (Wannier excitons are found in semiconductor crystals with small energy gaps and high dielectric constant).

In quantum mechanics, the positions of electrons and holes are described as wavefunctions or probability distributions. The exciton has a certain size, determined by the combined probability disctribution functions, and if this size exceeds the particle diameter, quantum confinement occurs. The size limit for quantum confinement is given by the diameter of the bulk Bohr exciton, which can be calculated from the Schrödinger equation. However it can be approximated from the modified version of the De Broglie wavelength equation considering its effective mass m^*:

$$\lambda_B = \frac{h}{p} = \frac{\hbar}{m^* \omega} \tag{3.11}$$

where λ_B is the de Broglie wavelength, $\hbar$ the reduced Planck constant and ω the angular frequency of the particle.

Material	ϵ_r	m_e^*	m_h^*
(Free electron mass $m_e = 9.11 \times 10^{-16} \ kg$)			
(Dielectric constant of vaccuum $\epsilon_0 \simeq 8.854 \times 10^{-12} \ A^2 s^4 kg^{-1} m^{-3}$)			
Silicon (Si) (4.2 K)	11.7	1.08 m_e	0.56 m_e
Germanium (Ge)	16.4	0.55 m_e	0.37 m_e
Gallium arsenide (GaAs)	$11.1 - 12.4$	0.067 m_e	0.45 m_e
Indium antimonide (InSb)	15.9 (at $77K$)	0.013 m_e	0.6 m_e
Zinc oxide (ZnO)	—	0.19 m_e	1.21 m_e
Zinc selenide (ZnSe)	—	0.17 m_e	1.44 m_e

Table 3.1: Relative dielectric constant (ϵ_r) measured at $290K$ [22] and effective mass of charge-carries for some common semiconductors [23], m_e^* and m_h^* respectively for the electron and hole effective mass

Nanocrystal contain many fewer atoms than found in the bulk, and as atoms are removed, charge screening effects are reduced. The effective mass declines and the de Broglie wavelength can become extremely large, up to several nanometers and makes the nanocrystal excited with much less energy than an atom. For cadmium sulfide (CdS) and cadmium telluride (CdTe), these wavelengths are 5.5 nm and 7.5 nm [20]. For particles that are confined within sizes smaller than this wavelength, the excitons "feels" restricted. Thus the nanocrystal will display a band gap and associated (optical and electrical) quantum effects proportional to its size.

Energy spectrum of semiconductor quantum dots An additional feature to the transition from bulk crystals to nanocrystals is a radical change in the energy spectrum of the free carriers. It changes when the diameter d of the crystal becomes comparable to the de Broglie wavelength of electrons in the crystal. Motion in the direction accross the nanocrystal can be assumed bounded, and the energy spectrum in this direction becomes discrete (Figure 3.3). Bulk semiconductor materials are characterized by bands of allowed potential energy values. An electron in the ground state may occupy any state within the valence band; while electrons in the excited state may occupy any state in the conduction band 3.3a. The region between the two bands is forbidden. For an electron to be excited, it must absorb at least enough to be carried from the highest energy state in the vlence band to the lowest energy state in the conduction band. Energies below this minimum value (i.e. the band gap) will not produce an excited state. However, a continuum of values greater than the band gap will produce an excited state.

When we examine a system consisting of only two atoms, the molecular

(a) Bulk semiconductor **(b)** Molecular material **(c)** Quantum dot
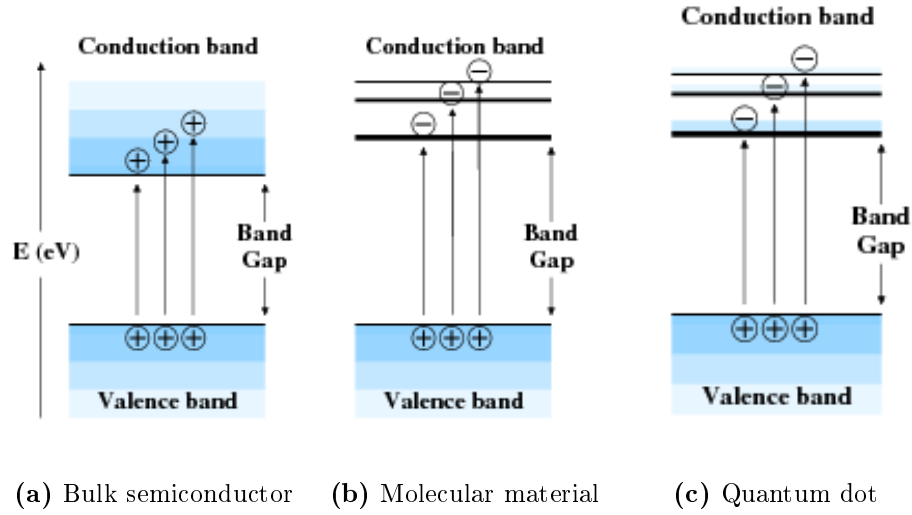
Figure 3.3: Possible energy states as a function of the particle size.
(a) Bulk materials have continuous energy bands and absorb energy at a value greater than the band gap. (b) Molecular materials possess discrete energy lelvels and only absorb energy wuth certain values. Moreover the band gap is greater than that of a bulk materail as a result of shrinking and splitting of the energy bands. (c) Quantum dots lie between the extremes (3.3a,3.3b). They possess discrete energy bands and absorb energy in discrete intervals. The band gap is greater than that of a molecular material.

orbitals formed create discrete potential energy states (Figure 3.3b). Electrons will only be excited if energy is absorbed in discrete quantities. Other values are not permitted and will not produce excited states.

Quantum Dots occupy the interval between discrete and continuous energy levels (Figure 3.3c). As the number of atoms in the particle is reduced, the energy bands split and shrink, eventually collapsing to the discrete values of the atomic state. Thus electrons in quantum dots may be excited by energies in discrete intervals, rather than a continuum.

3.3   Optical properties

A lot of applications rely on the optical properties of (colloidal) quantum dots and the latter result from quantum confinement.

The electrical and optical energy of the band gap are equivalent through the following conversion:

$$\Delta E = \hbar \omega = \frac{2\pi hc}{\lambda} \tag{3.12}$$

where ΔE is the band gap difference (figure 3.3c), $\hbar$ is the reduced Planck's constant, c is the speed of light, λ and ω respectively the the wavelength and the angular frequency of the incident light. Thus the energy difference of the band gap is inversely proportional to the wavelength of the incident light. Nanoparticles will only absorb light of wevalengths shorter than that determined by the band gap value.

For example, CdS (bulk) has a band gap of 2.42 eV, which corresponds to a wavelength of 512 nm. So CdS (bulk) begins to adsorb light at 512 nm and absorbs continuously into the UV (e.g. shorter wavelengths/higher energies). As particle size declines, the band gap increases and the absorbance starts at shorter wavelengths (Figure 3.4).

The influence of particle size on optical properties is not limited to absorbance. Particle fluorescence is also a function of the band gap. After an electron is excited, some of its energy is lost to atomic vibrations, satisfying the second law of thermodynamics. Typically, this energy is converted to heat. When the electron decays into the ground state, it will emit light, at a longer wavelength because of this energy loss (Figure 3.5a). As the band gap decreases, a smaller amount of energy is dissipated through fluorescent emission to return to the ground state, and the wavelength of emitted light will shift to the red (Figure 3.5b). Because the band gap is inversely proportional to nanocrystal size, larger nanocrystals display red-shifted emission. Additionally, the energy lost to heat decreases in a size-dependant manner.
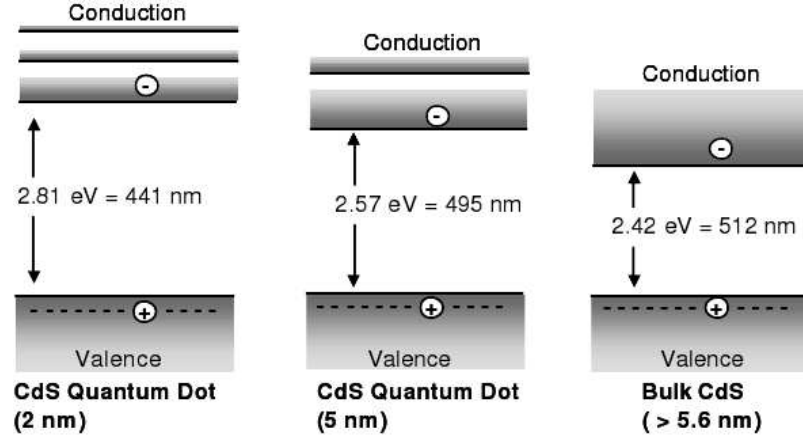
Figure 3.4: Band gap energy and optical absorption as a function of the crystal size. The band gap (eV) increases with decreasing nanoparticle size. Band gap is inversely related to the start in absorbance (λ) through the relationship $E = hc/\lambda$. Therefore smaller particles begin to absorb at shorter wavelengths [24].

3.4 Electronic properties/Manipulation of quantum dots

Electron-transfer between materials   Quantum confinement also affects the electrical properties of nanocrystals. Since gap energies are size dependent, electrical properties that depend on this difference will display size dependence as well. One such property is electron transfer. Electrons with no additional energy added prefer to move to lower energy states within a given material. Because there are no energy states in the band gap, the electron will decay until it reaches the lowest state in the conduction band, and then return to the valence band through another mechanism (i.e. electron-hole recombination, non-radiative energy loss, etc). However, if the electron encounters a material with lower available energy states (i.e. lower conduction band); it can transfer its electron to that material (Figure 3.6). This process is dependant upon the band gap. As the band gap increases, excited electrons occupy higher energy levels, and can decay to a greater number of lower state values. As a result of size-tunable band gaps within the particle, electron transfer can be optimized to many materials.

Single electron transport in quantum dots: Single-electron tunneling and Coulomb blockade   Electron transport through a quantum dot is studied by connecting the quantum dot to surrounding reservoirs (Figure 3.7). The fact that the charge on the electron island is quantized in units of the elementary charge
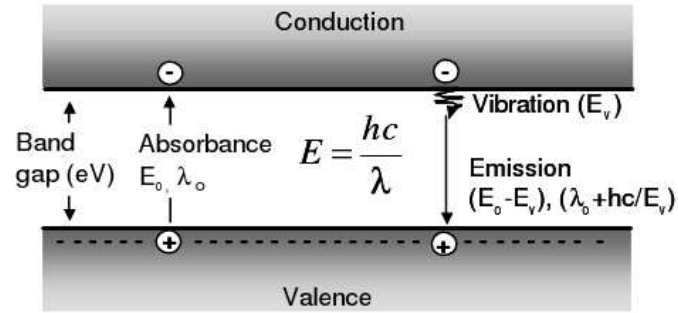
(a) Fluorescence and red-shift of λ due to energy loss.
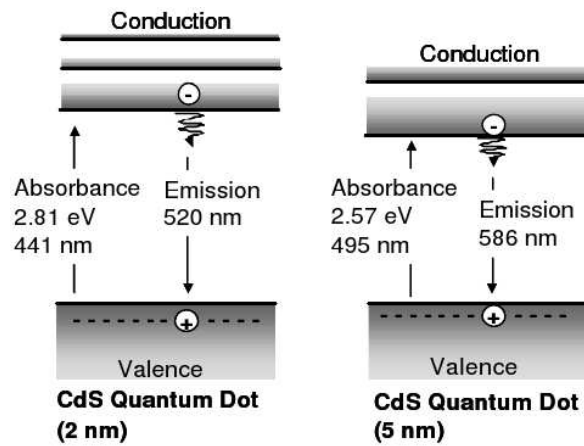
(b) Red-shifted emission due to crystal size.

Figure 3.5: Fluorescent emission and particle band gap, functions of the crystal size.
(a) Photon absorption creates an excited electron. This electron loses some energy to heat; then decays to ground, emitting a photon. The emitted photon has a longer wavelength than the absorbed photon because of the energy lost to heat.
(b) As the band gap decreases, the particle will absorb at longer wavelengths. This will produce a red-shift in particle fluorescent emission.
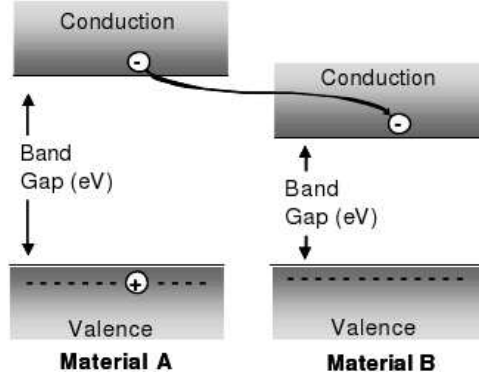
Figure 3.6: Electron transfer between materials with different band gaps.
If an excited electron in one material (A) encounters a second material (B) with a lower band gap energy, it can transfer its electron to that material.

e regulates transport through the quantum dot in the Coulomb blockade regime. Here the transport between the reservoirs and the dot occurs **via tunnel barriers**, which are thick enough that the transport is dominated by resonances due to quantum confinement in the dot. This requires a small transmission coefficient through the barriers, and thus the tunnel resistance has to be larger than the quantum resistance h/e^2. If the dot is fully decoupled from its environment, it confines a well defined number N of electrons. For weak coupling, deviations due to tunneling through the barriers are small, leading to discrete values in the total electrostatic energy of the dot. This energy can be estimated by $N(N-1)e^2/(2C)$, where C is the capacitance of the dot. Thus the addition of a single electron requires energy Ne^2/C, which is discretely spaced by the charging energy e^2/C. If this charging energy exceeds the thermal energy $k_B T$, the electrons cannot tunnel on and off the dot by thermal excitations alone, and transport can be blocked, which is referred to as a **Coulomb blockade**.

The two barries define the coupling of the channel to its surroundings. Figure 3.8d shows the result of the experiment, in which the conductance of the double-barrier channel was measured as a function of the gate voltage at different temperatures. One can see how the Coulomb blockade affects transport: clear peaks, equidistantly spaced, are separated by regions of zero conductance.

Following Kouwenhoven and McEuen (1999), figure 3.8a schematically illustrates an electron island connected to its environment by electrostatic barriers, the so-called source and drain contacts, and a gate to which one can apply a voltage V_g as depicted in figure 3.7.

In this example, the level structure of the quantum dot connected to source and drain by tunneling barriers is sketched schematically in Figures. 3.8(a)-(c). The chemical potential inside the dot, where the discrete quantum states are filled with N electrons [i.e. the highest solid line in Fig-
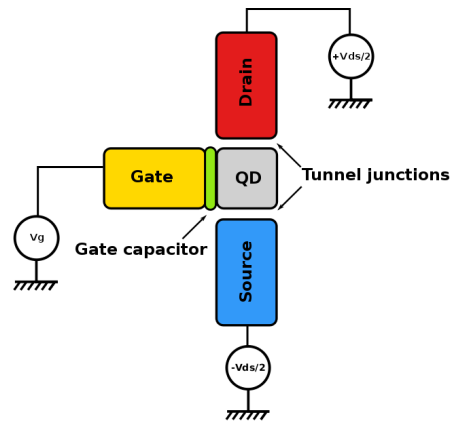
Figure 3.7: Schematic of a Single Electron Transistor (SET).
Setup for transport measurements on a lateral quantum dot. Because of the small size of the island or quantum dot (QD) in the middle of the two tunnel junctions the capacitance became very high and we see coulomb blockade effect.
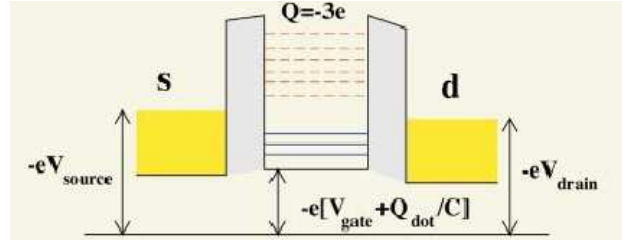
(a) Electron-transport blocked
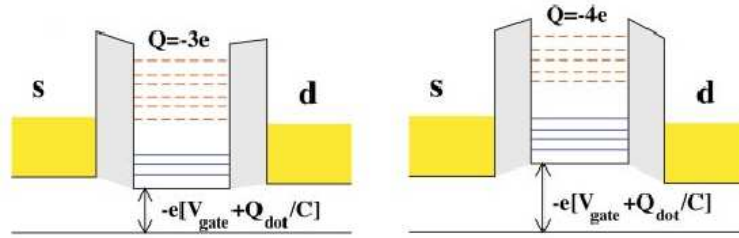
(b) Electron-transport allowed: maximum conductance
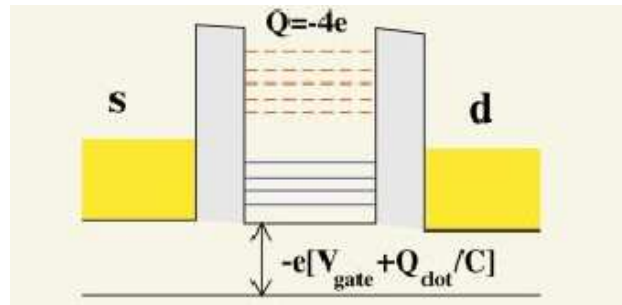
(c) Electron-transport blocked again
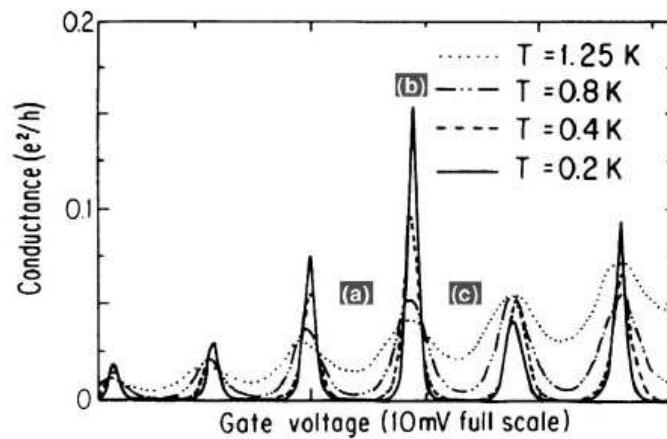
(d) Conductance of the double-barrier channel measured as a function of the gate voltage at different temperatures [25]

Figure 3.8: Single-electron transport in a quantum dot.
(a)-(c) Schematic picture of the level structures for single-electron transport (courtesy of A; Wacker). The solid lines represent the ionization potentials where the upper equals $\mu_{dot}(N)$, whereas the dashed lines refer to electron affinities, where the lowest one equals $\mu_{dot}(N+1)$. The gate bias increases from (a) to (c) [26].
(d) An example of the first measurements of Coulomb blockade as a function of the gate voltage.

ures. 3.8(a)-(c)], equals $\mu_{dot}(N) = E(N) - E(N+1)$, where $E(N)$ is the total groundstate energy (here at zero temperature).

When a bias voltage is applied to the source s and the drain d, the electrochemical potentials μ_s and μ_d are different, and a transport window $\mu_s - \mu_d = -eV_{ds}$ opens up, where e is the electron charge. In the linear regime the transport window $-eV_{ds}$ is smaller than the spacing of the quantum states, and only the ground state of the dot can contribute to the conductance. By changing the voltage on the back gate, one can achieve an alignment of $\mu_{dot(N+1)}$ with the transport window [Fig. 3.8b], and electrons can subsequently tunnel on and off the island at this particular gate voltage. This situation corresponds to a conductance maximum, as marked by the label (*b*) in Fig. 3.8d. Otherwise transport is blocked, as a finite energy is needed to overcome the charging energy. This scenario corresponds to zero conductance as marked by the labels (a) and (c) in Fig. 3.8. The mechanism of discrete charging and discharging of the dot leads to Coulomb blockade oscillations in the conductance as a function of gate voltage (as observed, for example, in Fig. 3.8d): at zero conductance, the number of electrons on the dot is fixed, whereas it is increased by one each time a conductance maximum is crossed. [26]

One can obtain spectroscopic information about the charge state and energy levels of the interacting quantum dot electrons by analyzing the precise shape of the Coulomb oscillations and the Coulomb staircase. In this way, single electron transport can be used as a spectroscopic tool [27].

3.5   Quantum dot in a magnetic field

In many experimental situations with quantum dots, the electrons in quantum dots are manipulated by an external magnetic field. This field is usually manipulated such that the magnetic field vector $\vec{B}$ is normal to the dot surface. For a typical quantum dot this results in a complicated spectrum of energy levels shown in figure 3.9.

The theoretical approach to the quantum dot given in the following chapter will serve as a basis to understand the spectrum of figure 3.9, even if the model used includes already many approximations.
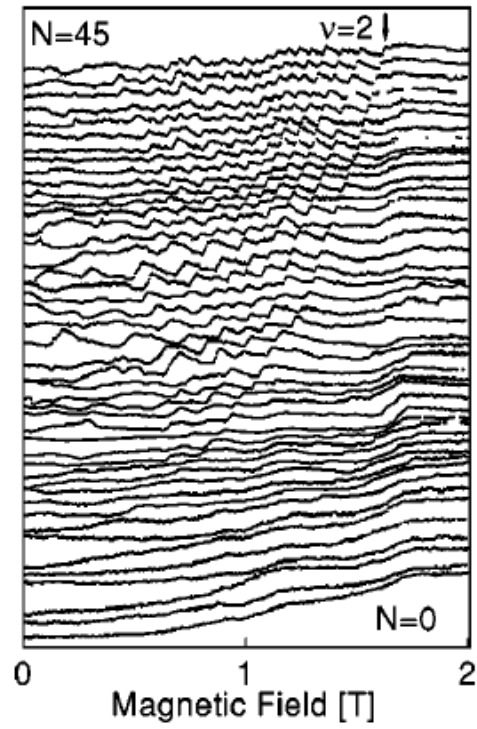
Figure 3.9: Additional energy spectrum as a function of a magnetic field. The magnetic field induces level crossings of single particle eigenstates which appear as cusps on the figure [28].

Chapter 4

Modelling of Quantum Dots

Quantum systems are governed by the Schrödinger equation (4th postulate of quantum mechanics):

$$H|\psi(t)\rangle = i\hbar\frac{d}{dt}|\psi(t)\rangle \tag{4.1}$$

where H is the quantum Hamilton operator (or Hamiltonian) and $|\psi(t)\rangle$ the state vector of the system.

In particular, the solutions to the stationary form of this equation determine many physical properties of the system at hand, such as the ground state energy of the system which is the ultimate result of our simulations. As expressed in section 2.3 we need a way to validate our model and we choose the ground state energy as physical quantity that can be compared with experiments and other numerical simulations.

Solving the Schrödinger equation in the Hamiltonian formalism obviously requires a definition of this Hamiltonian which translates as well as possible our knowledge of the system into equations. We must identify the different forces/fields applied to the system in order to include their respective "potentials" into the Hamiltonian.

In the case of a quantum dot, the Hamiltionan is basically characterized by the different forces applied to its constituants. This could be done by summing over all the interactions between electrons/nuclei that constitute the quantum dot. However, if the final objective is to perform fast predictions about the system, the complexity of such a model might quickly reach the limits of the computational resources.

So we prefer a simpler model in which the system is limited to the free charge-carries, i.e. by modelling a **confining potential** that traps them into the dot as well as an **interaction potential** that characterizes the repulsion between those electrons.

In the following, a discussion is made on possible models of those potentials. The derivation of a Hamiltonian is then given for electrons that repeal each other by a Coulomb interaction and trapped in a parabolic potential and ever more confined by applying or not an external magnetic field. We show finally that rescaling the problem with proper length and energy units leads to a simple form of the Hamiltonian even when applying an external magnetic field to the quantum dot.

4.1 Theoretical approximation of the quantum dot Hamiltonian

Two-body interaction potential   The interaction potential between two electrons is usually approximated proportional to the Coulomb repulsion in free space $V(\vec{r_i}, \vec{r_j}) = 1/r_{ij}$. For sake of simplicity and since it is still in use in most studies of quantum dots, we will stick to this approximation in this thesis. Nevertheless other studies have investigated other forms of potential. For example Johnson and Payne [29] assumed the interaction potential $V(\vec{r_i}, \vec{r_j})$ between particles i and j moving in the confining potential to saturate at small particle separation and to decrease quadratically with increasing separation. More recently, in order to investigate spin relaxation in quantum dots, Chaney and Maksym in [30] designed a more realistic confinement potential, electron-electron interactions, and screening where the parameters are obtained by fitting to experimental data.

The confining potential   Defining the second potential that confines those electrons appears as a bigger issue while modelling a quantum dot. Some numerical [31,32,33,34] and experimental [35,36,37] studies have shown that for a small number of electrons trapped, the harmonic oscillator potential is a good approximation, at least to first approximation. In [29], the bare (i.e. unscreened) confining potential $V(\vec{r_i})$ for the ith particle is also modelled to be parabolic (i.e. the harmonic oscillator potential). It has been shown theoretically that for electrons contained in a parabolic potential there is a strong absorption of far-infrared light at the frequency corresponding to the bare parabola [38, 39, 40, 41]. This theoretical prediction is consistent with some experimental measurements on quantum dots [42]. Further evidence that the bare potential in many quantum-dot samples is close to parabolic is provided by simple electrostatic models [43].

A more complicated relation between the interactions   Other studies tested different spherically symmetric confining potentials with different profiles ("soft" and "hard") on electrons in coupled QDs [44], and observed the resulting electron interaction. It shows really different behaviors of the electron interaction between the soft (Gaussian) and the hard (rectangular-like) confining potential. This means that an accurate model of the confining potential is strongly determined by the type and shape of the QD under study and produces also different type of electron interaction.

Motivation for our model   Since we are focusing on the limits of the Hartree-Fock method with respect to other techniques rather than an exhaustive study of different types of quantum dots, we choose in the rest of the thesis to model the single quantum dot by a definite number of electron N_e, trapped by a pure isotropic harmonic oscillator potential and repealing each other with a two-body Coulomb interaction. Only closed shell systems are studied, meaning that the number of electrons present in the quantum dot are filling all single particle states until the Fermi level. This really simplifies the problem since all combinations of single particle states are reduced to one Slater determinant as detailed in 5.3.2.

4.2   General form of $\hat{H}$ with explicit physical interactions

In this section we derive the Hamiltonian of the quantum dot model with and without external magnetic field in order to show that the interaction with the external magnetic field will basically result in a modified harmonic oscillator frequency and a shift of the energy proportional to the strength of the field.

4.2.1   Electrons trapped in an harmonic oscillator potential

We consider a system of electrons confined in a pure isotropic harmonic oscillator potential $V(\vec{r}) = m^*\omega_0^2 r^2/2$, where m^* is the effective mass of the electrons in the host semiconductor (as defined in section 3.2), ω_0 is the oscillator frequency of the confining potential, and $\vec{r} = (x, y, z)$ denotes the position of the particle.

The Hamiltonian of a single particle trapped in this harmonic oscillator

potential simply reads

$$\hat{H} = \frac{\mathbf{p}^2}{2m^*} + \frac{1}{2}m^*\omega_0^2\|\mathbf{r}\|^2 \tag{4.2}$$

where $\mathbf{p}$ is the canonical momentum of the particle.

When considering several particles trapped in the same quantum dot, the Coulomb repulsion between those electrons has to be added to the single particle Hamiltonian which gives

$$\hat{H} = \sum_{i=1}^{N_e} \left(\frac{\mathbf{p_i}^2}{2m^*} + \frac{1}{2}m^*\omega_0^2\|\mathbf{r_i}\|^2 \right) + \frac{e^2}{4\pi\epsilon_0\epsilon_r} \sum_{i<j} \frac{1}{\|\mathbf{r_i} - \mathbf{r_j}\|}, \tag{4.3}$$

where N_e is the number of electrons, $-e$ $(e > 0)$ is the charge of the electron, ϵ_0 and ϵ_r are respectively the free space permitivity and the relative permitivity of the host material (also called dielectric constant), and the index i labels the electrons.

4.2.2   Electrons trapped in an harmonic oscillator potential in the presence of an external magnetic field

Let's assume a static magnetic field $\overrightarrow{B}$ along the z axis.

Ignoring for now the spin-dependent terms, the Hamiltonian of those electrons in an magnetic field now reads [45]

$$\hat{H} = \sum_{i=1}^{N_e} \left(\frac{(\mathbf{p_i} + e\mathbf{A})^2}{2m^*} + \frac{1}{2}m^*\omega_0^2\|\mathbf{r_i}\|^2 \right) + \frac{e^2}{4\pi\epsilon_0\epsilon_r} \sum_{i<j} \frac{1}{\|\mathbf{r_i} - \mathbf{r_j}\|}, \tag{4.4}$$

$$= \sum_{i=1}^{N_e} \left(\frac{\mathbf{p_i}^2}{2m^*} + \frac{e}{2m^*}(\mathbf{A} \cdot \mathbf{p_i} + \mathbf{p_i} \cdot \mathbf{A}) + \frac{e^2}{2m^*}\mathbf{A}^2 + \frac{1}{2}m^*\omega_0^2\|\mathbf{r_i}\|^2 \right) \tag{4.5}$$

$$+ \frac{e^2}{4\pi\epsilon_0\epsilon_r} \sum_{i<j} \frac{1}{\|\mathbf{r_i} - \mathbf{r_j}\|}, \tag{4.6}$$

where $\mathbf{A}$ is the vector potential defined by $\mathbf{B} = \nabla \times \mathbf{A}$.

In coordinate space, $\mathbf{p_i}$ is the operator $-i\hbar\nabla_i$ and by letting the Hamiltonian acting on the total wave function $\Psi(\mathbf{r})$ in the Schrödinger equation, we obtain the following operator acting on $\Psi(\mathbf{r})$

$$\mathbf{A} \cdot \mathbf{p_i} + \mathbf{p_i} \cdot \mathbf{A} = -i\hbar\left(\mathbf{A} \cdot \nabla_i + \nabla_i \cdot \mathbf{A}\right)\Psi \tag{4.7}$$

$$= -i\hbar\left(\mathbf{A} \cdot (\nabla_i\Psi) + \nabla_i \cdot (\mathbf{A}\Psi)\right) \tag{4.8}$$

We note that using the product rule and the Coulomb gauge $\nabla \cdot \mathbf{A} = 0$ (by choosing the vector potential as $\mathbf{A} = \frac{1}{2}\mathbf{B} \times \mathbf{r}$), $\mathbf{p_i}$ and ∇_i commute and we obtain

$$\nabla_i \cdot (\mathbf{A}\Psi) = \mathbf{A} \cdot (\nabla_i\Psi) + \underbrace{(\nabla_i \cdot \mathbf{A})}_{0}\Psi = \mathbf{A} \cdot (\nabla_i\Psi) \tag{4.9}$$

This leads us to the following Hamiltonian:

$$\hat{H} = \sum_{i=1}^{N_e} \left(-\frac{\hbar^2}{2m^*}\nabla_i^2 - i\hbar\frac{e}{m^*}\mathbf{A} \cdot \nabla_i + \frac{e^2}{2m^*}\mathbf{A}^2 + \frac{1}{2}m^*\omega_0^2\|\mathbf{r_i}\|^2 \right) \tag{4.10}$$

$$+ \frac{e^2}{4\pi\epsilon_0\epsilon_r}\sum_{i<j} \frac{1}{\|\mathbf{r_i} - \mathbf{r_j}\|}, \tag{4.11}$$

The linear term in $\mathbf{A}$ becomes, in terms of $\mathbf{B}$:

$$\frac{-i\hbar e}{m^*}\mathbf{A} \cdot \nabla_i = -\frac{i\hbar e}{2m^*}(\mathbf{B} \times \mathbf{r_i}) \cdot \nabla_i \tag{4.12}$$

$$= \frac{-i\hbar e}{2m^*}\mathbf{B} \cdot (\mathbf{r_i} \times \nabla_i) \tag{4.13}$$

$$= \frac{e}{2m^*}\mathbf{B} \cdot \mathbf{L} \tag{4.14}$$

where $\mathbf{L} = -i\hbar(\mathbf{r_i} \times \nabla_i)$ is the orbital angular momentum operator of the electron i.

If assuming the electrons confined in the xy-plane, the quadratic term in $\mathbf{A}$ appearing in 4.10 can be written in the form

$$\frac{e^2}{2m^*}\mathbf{A}^2 = \frac{e^2}{8m^*}(\mathbf{B} \times \mathbf{r})^2 \tag{4.15}$$

$$= \frac{e^2}{8m^*}B^2 r_i^2 \tag{4.16}$$

Until this point we have not taken into account the intrinsic magnetic moment of the electrons. These intrinsic magnetic moment, due to the electron spin in the host material, is given by

$$\mathcal{M}_s = -g_s^*\frac{e}{2m^*}\mathbf{S} \tag{4.17}$$

where $\mathbf{S}$ is the spin operator of the electron and g_s^* its effective spin gyro-magnetic ratio (or efffective *g-factor* in the host material).We see that the spin magnetic moment $\mathcal{M}_s$ gives rise to an additional interaction energy [45], linear in the magnetic field,

$$\hat{H}_s = -\mathcal{M}_s \cdot \mathbf{B} = g_s^*\frac{e}{2m^*}BS_z = g_s^*\frac{\omega_c}{2}S_z \tag{4.18}$$

where $\omega_c = eB/m^*$ is known as the cyclotron frequency.

The final Hamiltonian reads

$$\hat{H} = \sum_{i=1}^{N_e} \left(\frac{-\hbar^2}{2m^*}\nabla_i^2 + \overbrace{\frac{1}{2}m^*\omega_0^2\|\mathbf{r_i}\|^2}^{\substack{\text{Harmonic ocscillator}\\\text{potential}}} \right) + \overbrace{\frac{e^2}{4\pi\epsilon_0\epsilon_r}\sum_{i<j}\frac{1}{|\mathbf{r_i}-\mathbf{r_j}|}}^{\substack{\text{Coulomb}\\\text{interactions}}}$$

$$+ \underbrace{\sum_{i=1}^{N_e}\left(\frac{1}{2}m^*\left(\frac{\omega_c}{2}\right)^2\|\mathbf{r_i}\|^2 + \frac{1}{2}\omega_c\hat{L}_z^{(i)} + \frac{1}{2}g_s^*\omega_c\hat{S}_z^{(i)} \right)}_{\substack{\text{single particle interactions}\\\text{with the magnetic field}}}, \qquad (4.19)$$

4.2.3 Scaling the problem: Dimensionless form of $\hat{H}$

In order to simplify the computation, the Hamiltonian can be rewritten on dimensionless form. For this purpose, let's introduce some constants:

- the oscillator frequency $\omega = \omega_0\sqrt{1+\omega_c^2/(4\omega_0^2)}$,

- an new energy unit $\hbar\omega$,

- and a new length unit, the oscillator length defined by $l = \sqrt{\hbar/(m^*\omega)}$, also called the characteristic length unit.

Let's rewrite the Hamiltonian in dimensionless units using:

$$\mathbf{r} \longrightarrow \frac{\mathbf{r}}{l}, \quad \nabla \longrightarrow l\,\nabla \quad \text{and} \quad \hat{L}_z \longrightarrow \hat{L}_z$$

Leading to the following Hamiltonian:

$$\hat{H} = \sum_{i=1}^{N_e}\left(-\frac{1}{2}\nabla_i^2 + \frac{1}{2}r_i^2 \right) + \overbrace{\frac{e^2}{4\pi\epsilon_0\epsilon_r}\frac{1}{\hbar\omega l}}^{\substack{\text{Dimensionless}\\\text{confinement}\\\text{strength }(\lambda)}}\sum_{i<j}\frac{1}{r_{ij}}$$

$$+ \sum_{i=1}^{N_e}\left(\frac{1}{2}\frac{\omega_c}{\hbar\omega}\hat{L}_z^{(i)} + \frac{1}{2}g_s^*\frac{\omega_c}{\hbar\omega}\hat{S}_z^{(i)} \right), \qquad (4.20)$$

Lengths are now measured in units of $l = \sqrt{\hbar/(m^*\omega)}$, and energies in units of $\hbar\omega$.

A new dimensionless parameter $\lambda = l/a_0^*$ (where $a_0^* = 4\pi\epsilon_0\epsilon_r\hbar^2/(e^2m^*)$ is the effective Bohr radius) describes the strength of the electron-electron interaction. Large λ implies strong interaction and/or large quantum dot [46].
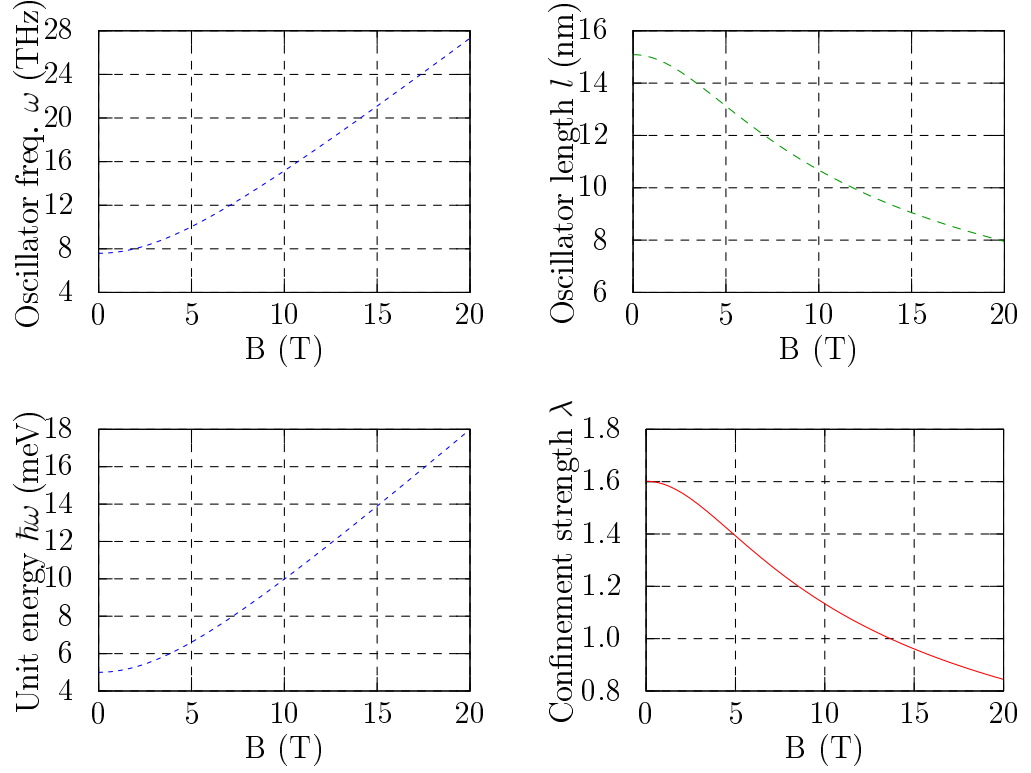
Figure 4.1: Typical values for the oscillator frequency ω, the oscillator length l, the energy unit $\hbar\omega$ and the dimensionless confinement strength λ as a function of the magnetic field strength in GaAs semiconductors assuming: $\hbar\omega_0 = 5 \times 10^{-3} eV$ **??**, $\epsilon_r \simeq 12$ and $m^* = 0.067\, m_e$

Since both $\hat{L}_z$ and $\hat{S}_z$ commute with the Hamiltonian we can perform the calculations separately in subspaces of given quantum numbers L_z and S_z. Figure 4.1 displays values of the different parameters as a function of the magnetic field strength for a particular type of semiconductor: Gallium arsenide (GaAs) with know characteristics given in table 3.1.

The simplified dimensionless Hamiltonian becomes

$$\hat{H} = \sum_{i=1}^{N_e} \left[-\frac{1}{2}\nabla_i^2 + \frac{1}{2}r_i^2 \right] + \lambda \sum_{i<j} \frac{1}{r_{ij}} + \sum_{i=1}^{N_e} \left(\frac{1}{2}\frac{\omega_c}{\hbar\omega}L_z^{(i)} + \frac{1}{2}g_s^*\frac{\omega_c}{\hbar\omega}S_z^{(i)} \right), \quad (4.21)$$

The last term which is proportional to the magnetic field involves only the quantum numbers L_z and S_z and not the operators themselves [46]. Therefore their contributions can be added when the remaining part has

been solved and the squizzing effect of the magnetic field being included simply in the parameter λ. This brings us to the simple and general form of the Hamiltonian to study:

$$\hat{H} = \sum_{i=1}^{N_e} \left(-\frac{1}{2}\nabla_i^2 + \frac{1}{2}r_i^2 \right) + \lambda \sum_{i<j} \frac{1}{r_{ij}}. \qquad (4.22)$$

Chapter 5

Many-body treatment: the Hartree-Fock method

A many-body system with interactions is generally very difficult to solve exactly, except for extremely simple cases. It is the same when it comes to quantum dots that can simply be seen as a many-electron problem.

In the first section of this chapter we will detail the derivation of exact solutions for the two-electrons quantum dot for some particular parameters. Then some numerical approximations techniques are used in order to get information about the properties of the system as close as possible from their real values. In this thesis we focus on the ground state energy of quantum dots (i.e. the energy of the system at rest without external time-dependent excitations). And for this purpose, several many-body techniques can be used with of course different accuracy and efficiency.

We will of course detail the Hartree-Fock method which is a major part of this thesis and compare its results to other *Ab initio* methods such as perturbation theory, variational Monte-Carlo or large scale diagonalisation.

5.1 Analytical solutions of some particular cases

[Exact solution for 2 electrons in Simen thesis p.4 of paper 2]

5.1.1 Non-interacting particles trapped in a pure HO potential

5.1.2 Two-electrons quantum dot with/without magnetic field

In solving many-body problems (i.e. many-particle problems), it common to hear in this field that "many starts at two". Analytical solution of the two-

electrons QD [Taut 1993- 2D with B field + 3D without B field]

[transition for next part: there is not many exact solutions for the study of many-electron QD and for those that exist, they require particular restrictions for the model under study. So numerical methods appear as the only to implement a more general form of the QD model and to solve the many-body problem. The next section introduces the Hartree-Fock method as one possible numerical technique with its pros and cons wrt to other methods.]

5.2   Ab initio many-body techniques

[Introduce the Hartree-Fock method as one possible ab initio technique]
Ab-initio methods: HF, VMC, CI, PDE (pros and cons).
What other properties that the ground state energy can I expect to get from the methods? since HF is a mean-field approximation, we can't for example determine the charge localization of the system.

The term *"ab initio"* indicates that the calculation is from first principles and that no empirical data is used.

The simplest type of *ab initio* electronic structure calculation is the Hartree-Fock (HF) scheme, in which the instantaneous Coulombic electron-electron repulsion is not specifically taken into account. Only its average effect (mean field) is included in the calculation. This is a variational procedure; therefore, the obtained approximate energies, expressed in terms of the system's wave function, are always equal to or greater than the exact energy, and tend to a limiting value called the Hartree-Fock limit as the size of the basis is increased [47].

Many types of calculations begin with a Hartree-Fock calculation and subsequently correct for electron-electron repulsion, referred to also as electronic correlation. Configuration Interaction (CI) and Coupled cluster theory (CC) may be some examples of these post-Hartree-Fock methods.

Figure 5.2 presents a diagram illustrating electron correlation energy in terms of various levels of theory. As shown on the figure, HF may present the worse approximation to the exact energy of a many-body system, but its simplicity is on all fours with its computational simplicity (i.e.špeed) compared to other methods.

In some cases, particularly for bond breaking processes, the Hartree-Fock method is inadequate and this single-determinant reference function is not a good basis for post-Hartree-Fock methods. It is then necessary to start with a wave function that includes more than one determinant.

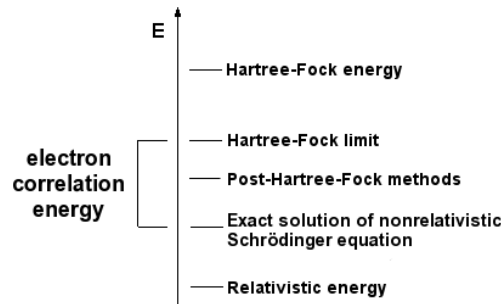A method that avoids making the variational overestimation of HF in

Figure 5.1: Electron correlation energy in terms of various levels of theory of solutions for the Schrödinger equation. (K. Langner, 2005)

the first place is Quantum Monte Carlo (QMC), in its variational, diffusion, and Green's function forms. These methods work with an explicitly correlated wave function and evaluate integrals numerically using a Monte Carlo integration. Such calculations can be very time-consuming, but they are probably the most accurate methods known today.

Ab initio electronic structure methods have the advantage that they can be made to converge to the exact solution, when all approximations are sufficiently small in magnitude. In particular, configuration interaction, where all possible configurations are included (called "Full CI") tends to the exact non-relativistic solution of the Schrödinger equation, and therefore to the best possible solution in principle.

However Full CI is often impossible for anything but the smallest systems. The convergence, is usually not monotonic, and sometimes the smallest calculation gives the best result for some properties.

Then the downside of ab initio methods is their computational cost. They often take enormous amounts of computer time, memory, and disk space. The HF method scales nominally as N^4 (N being the number of basis functions), i.e.ã calculation twice as big takes 16 times as long to complete. However in practice it can scale closer to N^3 as the program can identify zero and extremely small integrals and neglect them. Correlated calculations scale even less favorably - MP2 as N^5; MP4 as N^6 and coupled cluster as N^7. Density functional theory (DFT) methods scale in a similar manner to Hartree-Fock but with a larger proportionality term. Thus DFT calculations are always more expensive than an equivalent Hartree-Fock calculation [48]

[FIND BETTER SOURCE THAN WIKIPEDIA TO PROVIDE RESULTS ON THE COMPUTATIONAL COMPLEXITY]. Look at Simen's derivation for computing the error of FCI and looking at the biggest system that can be studied wrt the limit in memory of a supercomputer.

Many [49]

5.3   Time-independent Hartree-Fock Theory

say something on restricte, unrestricted HF. $=>$ descriptions in Morten's slides: FYS4410. s.386/412 $http://en.wikipedia.org/wiki/Mean_field_theory$ $=$ derivation of HF equations. These equations will be different in the 2 simulations that will be made:

1. varying directly the wave function as in project 1 (Numerov's algo, Shooting method/Green's function/Wronskian...)

2. varying the coefficient of the HO wf which leads to solving a linear system How good is the Hartree-Fock approximation? (Moshinsky1969 p.77 [50]).

The Hartree-Fock method is a minimization method based on a mathematical technique known as the Lagrange multipliers, where the functional to minimize is the energy of the system.

Since the energy which is an expectation value of the Hamiltonian can be written explicitly as an integral, we will review an approximated method, the Variational method and how it minimizes such a functional based on Lagrange multipliers. The *variational method* (or *variational calculus* or *calculus of variations*) is really useful in obtaining the bound state energies and wave functions of a time-independent Hamiltonian $\hat{H}$. Then the approximations applied to the wave function and the energy functional of the system are detailled when dealing with a many-body problem. The variational method and those approximations lead us to the derivation of the *Hartree-Fock method*, a mean-field variational method also categorized as a *self-consistent method*,.

[DETAILS ON MEAN-FIELD THEORY (MFT) found on wiipedia] $http://en.wikipedia.org/wiki/Mean_field_theory$ The n-body system is replaced by a 1-body problem with a chosen good external potential (i.e. field). The external field replaces the interaction of all the other particles to an arbitrary particle. The great difficulty (e.g. when computing the partition function of the system) is the treatment of combinatorics generated by the interaction terms in the Hamiltonian when summing over all states. The goal of mean field theory (MFT, also known as self-consistent field theory) is to resolve these combinatorial problems.

The main idea of MFT is to replace all interactions to any one body with an average or effective interaction. This reduces any multi-body problem into an effective one-body problem. The ease of solving MFT problems means that some insight into the behavior of the system can be obtained at a relatively low cost.

In field theory, the Hamiltonian may be expanded in terms of the magnitude of fluctuations around the mean of the field. In this context, MFT can be viewed as the "zeroth-order" expansion of the Hamiltonian in fluctuations. Physically, this means an MFT system has no fluctuations, but this coincides with the idea that one is replacing all interactions with a "mean field". Quite often, in the formalism of fluctuations, MFT provides a convenient launch-point to studying first or second order fluctuations.

In general, dimensionality plays a strong role in determining whether a mean-field approach will work for any particular problem. In MFT, many interactions are replaced by one effective interaction. Then it naturally follows that if the field or particle exhibits many interactions in the original system, MFT will be more accurate for such a system. This is true in cases of high dimensionality, or when the Hamiltonian includes long-range forces. The Ginzburg criterion is the formal expression of how fluctuations render MFT a poor approximation, depending upon the number of spatial dimensions in the system of interest.

5.3.1 Variational Calculus and Lagrange Multipliers

As we have seen in the previous part, in most cases we must resort to computers to determine the solutions of the Shrödinger equation. It is of course possible to integrate the equation using discretisation methods, but in most realistic electronic structure calculations we would need huge numbers of grid points, leading to high computer time and memory requirements. The variational method on the other hand enables us to solve the Schrödinger equation much more efficiently in many cases [51].

As for the method of Lagrange multipliers in mathematical optimization (more details about this method in appendix B.1), the calculus of variations provides a strategy for finding the stationnary points of a function subject to some constraints. Maxima and minima can be found this way when the function is differentiable.

More specifically the calculus of variations involves problems where the quantity to be minimized or maximized (the functional) is an integral.

In the general case we have an integral of the type

$$E[\Phi] = \int_a^b f(\Phi(x), \frac{\partial \Phi}{\partial x}, x) dx,$$

where E is the quantity which is sought minimized or maximized.

The problem is that although f is a function of the variables Φ, $\partial \Phi / \partial x$ and x, the exact dependence of Φ on x is not known. This means again that even though the integral has fixed limits a and b, the path of integration

is not known. In our case the unknown quantities are the single-particle wave functions and we wish to choose an integration path which makes the functional $E[\Phi]$ stationary. This means that we want to find minima, or maxima or saddle points. In physics we search normally for minima.

Our task is therefore to find the minimum of $E[\Phi]$ so that its variation δE is zero subject to specific constraints. In our case the constraints appear as the integral which expresses the orthogonality of the single-particle wave functions. The constraints can be treated via the technique of the Lagrange multipliers.

In the following, we will be more specific with the form of the functional which now reads

$$E[\Phi] = \frac{\langle \Phi | H | \Phi \rangle}{\langle \Phi | \Phi \rangle} = \frac{\int \Phi^* H \Phi d\tau}{\int \Phi^* \Phi d\tau} \tag{5.1}$$

where the integration is extended over the full range of all the coordinates of the system.

We denote by E_n the eigenvalues of the Hamiltonian and by Ψ_n the corresponding orthonormal eigenfunctions, and assume that $\hat{H}$ has at least one discrete eigenvalue. It is clear that if the function Φ is identical to one of the exact eigenfunctions Ψ_n of $\hat{H}$; then $E[\Phi]$ will be identical to the corresponding exact eigenvalue E_n.

In the following, we will show that:

1. any function Φ for which the functional $E[\Phi]$ is stationary is an eigenfunction of the discrete spectrum of $\hat{H}$.

2. using the method of the Lagrange multipliers and varying the functional $\langle \Phi | H | \Phi \rangle$ subject to the normalisation condition $\langle \Phi | \Phi \rangle = 1$, the Lagrange multiplier itself has the significance of an energy eigenvalue.

3. the functional $E[\Phi]$ gives an upper bound for the ground state energy, also known as the *variational principle.*

4. it is possible to solve the Schrödinger equation using the variational method.

Any function Φ for which the functional $E[\Phi]$ is stationary is an eigenfunction of $\hat{H}$ If Φ and an exact eigenfunction Ψ_n differ by an arbitrary infinitesimal variation $\delta\Phi$,

$$\Phi = \Psi_n + \delta\Phi,$$

then the corresponding first-order variation of $E[\Phi]$ vanishes:

$$\delta E = 0, \tag{5.2}$$

and the eigenfunctions of $\hat{H}$ are solutions of the variational equation 5.2.

To prove this statement, we note re-writting the functional as

$$E[\Phi] \int \Phi^* \Phi d\tau = \int \Phi^* H \Phi d\tau,$$

and varying it gives:

$$\delta E \int \Phi^* \Phi d\tau + E \int \delta \Phi^* \Phi d\tau + E \int \Phi^* \delta \Phi d\tau = \int \delta \Phi^* H \Phi d\tau + \int \Phi^* H \delta \Phi d\tau.$$

Since $\Phi | \Phi$ is assumed to be finite and non-vanishing, we see that the variational equation 5.2 is equivalent to

$$\int \delta \Phi^* (H - E) \Phi d\tau + \int \Phi^* (H - E) \delta \Phi d\tau = 0. \qquad (5.3)$$

Although the variations $\delta \Phi$ and $\delta \Phi^*$ are not independent, they may in fact be treated as such, so that the individual terms in 5.3 can be set equal to zero. TO see how this comes about, we replace the arbitrary variation $\delta \Phi$ by $i\delta \Phi$ in 5.3 so tht we obtain

$$-i \int \delta \Phi^* (H - E) \Phi d\tau + i \int \Phi^* (H - E) \delta \Phi d\tau = 0. \qquad (5.4)$$

By combining 5.3 with 5.4 we then obtain the two equations

$$\begin{cases} \delta \Phi^* (H - E) \Phi d\tau = 0 \\ \Phi^* (H - E) \delta \Phi d\tau = 0 \end{cases} \qquad (5.5)$$

which is the desired result. Using the fact that $\hat{H}$ is Hermitian, we see that the two equation 5.5 are equivalent to the Schödinger equation $(H - E[\Phi])\Phi = 0$.

Thus any function $\Phi = \Psi_n$ for which the functional 5.1 is stationary is an eigenvalue of $\hat{H}$ corresponding to the eigenvalue $E_n = E[\Psi_n]$. It is worth stressing that if Φ and Ψ_n differ by $\delta \Phi$, the variational equation 5.2 implies that the leading term of the difference $E[\Phi] - E_n$ is quadratic in $\delta \Phi$. As a result, errors in the approximate energy are of second order in $\delta \Phi$ when the energy is calculated from the functional 5.1.

the Lagrange multiplier has the significance of an energy eigenvalue   We also remark that the functional 5.1 is independent of the normalisation and of the phase of Φ. In particular, it is often convenient to impose the condition

$\langle\Phi|\Phi\rangle = 1$. The above results may then be retrieved by varying the functional $\langle\Phi|H|\Phi\rangle = 1$ subject to the condition $\langle\Phi|\Phi\rangle = 1$, namely

$$\delta \int \Phi^* H \Phi d\tau = 0, \quad \int \Phi^* \Phi d\tau = 1.$$

The constraint $\langle\Phi|\Phi\rangle = 1$ may be taken care of by introducing a Lagrange multiplier (as described in appendix B.1) which we denote by Σ.

We define the Lagrangian Λ as

$$\Lambda(\Phi, \Sigma) = \int \Phi^* H \Phi d\tau - \Sigma \left(\int \Phi^* \Phi d\tau - 1 \right),$$

so that the variational equation reads

$$\delta\Lambda(\Phi, \Sigma) = 0 \tag{5.6}$$

$$\delta \left[\int \Phi^* H \Phi d\tau - \Sigma \int \Phi^* \Phi d\tau \right] = 0, \tag{5.7}$$

or

$$\int \delta\Phi^* (H - \Sigma)\Phi d\tau + \int \Phi^* (H - \Sigma)\delta\Phi d\tau = 0,$$

This equation is identical to 5.3, and we see that the Lagrange multiplier $\Sigma = E$ has the significance of an energy eigenvalue.

the variational principle An important additional property of the functional 5.1 is that it provides an upper bound to the exact ground state E_0. To prove this result, we expand the arbitrary, normalisable function Φ in the complete set of orthonormal eigenfunctions Ψ_n of $\hat{H}$. This reads

$$\Phi = \sum_n a_n \Psi_n. \tag{5.8}$$

Substituing the expansion 5.8 into the functional 5.1, we find that

$$E[\Phi] = \frac{\sum_n |a_n|^2 E_n}{\sum_n |a_n|^2}, \tag{5.9}$$

where we have used the fact that $H\Psi_n = E_n\Psi_n$ and $\langle\Phi|\Phi\rangle = \sum_n |a_n|^2$. If we now subtract E_0, the lowest energy eigenvalue, from both sides of the functional 5.9 we have

$$E[\Phi] - E_0 = \frac{\sum_n |a_n|^2 (E_n - E_0)}{\sum_n |a_n|^2}. \tag{5.10}$$

Since $E_n \geq E_0$, the right-hand side of 5.10 is non-negative, so that

$$E_0 \leq E[\Phi] \tag{5.11}$$

and the functional $E[\Phi]$ gives an upper-bound, or in order words a *minimum principle* for the ground state energy [45].

Solving the Schrödinger equation using the variational method   In the variational method, the possible solutions (i.e. the stationary states of the energy functional) are restricted to a subspace of the Hilbert space, and in this subspace we seek the "best possible" solution. An important example is linear variational calculus, in which the subspace is spanned by a set of basis vectors χ_i for $i = 1, \ldots, P$ where P is the size of the basis set. We take these to be orthonormal at first, that is,

$$\langle \chi_i | \chi_j \rangle = \delta_{ij}.$$

For an arbitrary state $|\Psi\rangle = \sum_i C_i |\chi_j\rangle$, the energy functional is given by

$$E = \frac{\langle \Psi | H | \Psi \rangle}{\langle \Psi | \Psi \rangle} = \frac{\sum_{i,j=1}^{R} C_i^* C_j H_{ij}}{\sum_{i,j=1}^{R} C_i^* C_j \delta_{ij}},$$

where $H_{ij} = \langle \chi_i | H | \chi_j \rangle$ is assumed to be known.

The stationary states follow from the condition that the derivative of this functional with respect to the C_i vanishes, which leads to

$$\sum_{j=1}^{R} (H_{ij} - E\delta_{ij})C_j = 0, \qquad for \quad i = 1, \ldots, R. \tag{5.12}$$

Equation 5.12 is then an eigenvalue problem which can be written in matrix notation as

$$\mathbf{HC} = \mathbf{EC}. \tag{5.13}$$

This is the Schrödinger equation, formulated for a finite, orthonormal basis.

The lowest eigenvalue of eq. 5.13 is always higher that or equal to the ground state energy, as we proved that the ground state is the minimal value assumed by the energy-functional in the full Hilbert space. If we restrict ourselves to a part of this space, then the minimum value of the energy functional must always be higher than or equal to the ground state of the full Hilbert space. Including more basis functions into our setm the subspace becomes larger and consequently the minimum of the energy functional will decrease (or stay the same). The behaviour of the spectrum found by solving 5.13 with increasing size of the basis set R is depicted in figure 5.2.
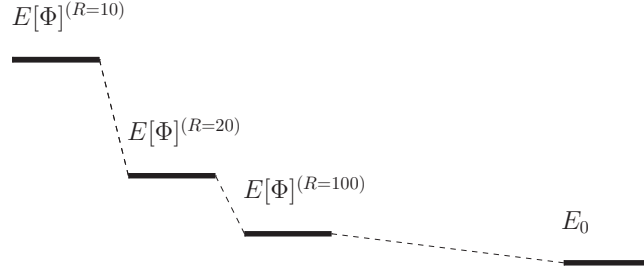
Figure 5.2: The behaviour of the ground state energy of eq. 5.12 with increasing basis set size R in linear variational calculus. The upper index is the number of states in the basis set.

Then variational approach discussed here provides a powerful method for obtaining approximate solutions of the wave function. But this might not be sufficient when dealing with a system made of many interacting particles, where more approximations have to be done about the wave function of the system in order to lead again to a simple eigenvalue problem.

5.3.2 Approximated wave function of the many-body system

The Schrodinger equation for a system of N electron reads:

$$\hat{H}(\mathbf{r_1}, \mathbf{r_2}, \ldots, \mathbf{r_N})\Psi_\eta(\mathbf{r_1}, \mathbf{r_2}, \ldots, \mathbf{r_N}) = E_\eta\Psi_\eta(\mathbf{r_1}, \mathbf{r_2}, \ldots, \mathbf{r_N}) \tag{5.14}$$

where the vector $\mathbf{r}_i$ represents the coordinates (spatial and spin) of a particle i, η stands for all the quantum numbers needed to classify a given N-particle state and Ψ_η is the corresponding eigenfunction.

The Hamiltonian can be written in the form

$$\hat{H} = \hat{T} + \hat{V}$$

where $\hat{T}$ represents the kinetic energy of the system

$$\hat{T} = \sum_{i=1}^{N} \frac{\mathbf{p_i^2}}{2m_i} = \sum_{i=1}^{N} \left(-\frac{\hbar^2}{2m_i}\nabla_i^2 \right) = \sum_{i=1}^{N} t(\mathbf{r_i})$$

while the operator $\hat{V}$ represents the potential energy given by

$$\hat{V} = \underbrace{\sum_{i=1}^{N} u(\mathbf{r_i})}_{\substack{\text{one-particle} \\ \text{interaction}}} + \underbrace{\sum_{i<j}^{N} v(\mathbf{r_i}, \mathbf{r_j})}_{\substack{\text{two-particles} \\ \text{interaction}}} = \underbrace{\sum_{i=1}^{N} \frac{1}{2}m\omega^2 r_i^2}_{\substack{\text{confining} \\ \text{potential}}} + \lambda^* \underbrace{\sum_{i<j}^{N} \frac{1}{\parallel \vec{r_i} - \vec{r_j} \parallel}}_{\substack{\text{Coulomb} \\ \text{repulsion}}} \tag{5.15}$$

where ω is the frequency of the harmonic oscillator potential and λ^* is the dimensionless parameter characterizing the interaction strength as defined in eq. (**??**).

Hereafter we use atomic units, viz. $\hbar=c=e=1$ with e the elementary charge and c the speed of light. This means that momenta and masses have dimension energy. In the last equation we have singled out an external one-body potential term u which is meant to represent an effective one-body field in which our particles move (i.e. the harmonic oscillator potential in our first approximation for the confining potential of the QD model) .

We have therefore assumed that a picture consisting of individual electrons is a viable starting point for wave function approximations. We can rewrite the Hamiltonian for N electrons as

$$\hat{H} = \hat{H}_0 + \hat{H}_1 = \sum_{i=1}^{N} \hat{h}_i + \lambda^* \sum_{i<j}^{N} \frac{1}{r_{ij}}, \tag{5.16}$$

where we have defined $r_{ij} = \| \vec{r_i} - \vec{r_j} \|$ and $\hat{h}_i = t(\mathbf{r_i}) + u(\mathbf{r_i})$.

The first term of the eq.(5.16), $\hat{H}_0$, is the sum of the N one-body Hamiltonians $\hat{h}_i$. Each individual Hamiltonian $\hat{h}_i$ contains the kinetic energy operator of an electron and its potential energy due to the confining potential. The potential energy term due to the harmonic oscillator potential defines the one-body field $u_i = u(\mathbf{r_i})$ of eq.(5.15). We have moved this term into the $\hat{H}_0$ part of the Hamiltonian, instead of keeping it in $\hat{V}$ as in eq.(5.15). The reason is that we will hereafter treat $\hat{H}_0$ as our non-interacting Hamiltonian. For a many-body wavefunction Ψ_η defined by an appropriate single-particle basis, we may solve exactly the non-interacting eigenvalue problem

$$\hat{H}_0\Psi_\eta = E_\eta\Psi_\eta,$$

with E_η being the non-interacting energy. This energy is defined by the sum over single-particle energies. In our model of the quantum dot, the single-particle energies are the harmonic oscillator single-particle energies in 2D or 3D respectively.

The second term of the eq.(5.16), $\hat{H}_1$, is the sum of the $N(N-1)/2$ two-body interactions between each pair of electrons. Note that the double sum carries a restriction $i < j$.

Irrespective of these approximations, there is a wealth of experimental evidence that these interactions have to obey specific symmetries. The total Hamiltonian should be translationally invariant. If angular momentum is conserved, the Hamiltonian is invariant under rotations. Furthermore, it is invariant under the permutation (interchange) of two particles. Since we deal with fermions, the total wave function is antisymmetric.

Let $\hat{P}$ be an operator which interchanges two particles. Due to the symmetries we have ascribed to our Hamiltonian, this operator commutes with the total Hamiltonian,

$$[\hat{H}, \hat{P}] = 0,$$

meaning that $\Psi_\eta(\mathbf{r_1}, \mathbf{r_2}, \ldots, \mathbf{r_N})$ is an eigenfunction of $\hat{P}$ as well, that is

$$\hat{P}_{ij}\Psi_\eta(\mathbf{r_1}, \mathbf{r_2}, \ldots, \mathbf{r_i}, \ldots, \mathbf{r_j}, \ldots, \mathbf{r_N}) = \beta\Psi_\eta(\mathbf{r_1}, \mathbf{r_2}, \ldots, \mathbf{r_j}, \ldots, \mathbf{r_i}, \ldots, \mathbf{r_N}),$$

where β is the eigenvalue of $\hat{P}$. We have introduce the suffix ij in order to indicate that we permute particles i and j. The Pauli principle tell us that the total wave function for a system of fermions has to be antisymmetric, resulting in the eigenvalue $\beta = -1$ [reference:Morten book??? chap.2 cite-mortenBook].

We approximate our many-body wave function with the product of single-particle wave functions. Since we assume that our Hamiltonian is time-independent, these single-particle wave functions are normally the eigenfunctions of a selected one-body Hamiltonian $\hat{h}_i$ acting on particle i.

In Hartree-Fock we approximate the exact eigenfunction[1] Ψ_λ by a trial wave function Φ built as a Slater determinant

$$\Phi(\mathbf{r_1}, \mathbf{r_2}, \ldots, \mathbf{r_N}, \alpha, \beta, \ldots, \sigma) = \frac{1}{\sqrt{N!}} \begin{vmatrix} \psi_\alpha(\mathbf{r}_1) & \psi_\beta(\mathbf{r}_2) & \ldots & \psi_\sigma(\mathbf{r}_N) \\ \psi_\alpha(\mathbf{r}_1) & \psi_\beta(\mathbf{r}_2) & \ldots & \psi_\sigma(\mathbf{r}_N) \\ \vdots & \vdots & \ddots & \vdots \\ \psi_\alpha(\mathbf{r}_1) & \psi_\beta(\mathbf{r}_2) & \ldots & \psi_\sigma(\mathbf{r}_N) \end{vmatrix},$$

(5.17)

where the variables $\mathbf{r_i}$ include the coordinates of spin and space of particle i, and $\alpha, \beta, \ldots, \sigma$ encompass all possible quantum numbers needed to specify a particular system. The single-particle function $\psi_\alpha(\mathbf{r_i})$ are eigenfunctions of the onebody Hamiltonian $\hat{h}_i$, that is

$$\hat{h}_i = h(\mathbf{r_i}) = t(\mathbf{r_i}) + u(\mathbf{r_i}),$$

with eigenvalues

$$\hat{h}_i\psi_\alpha(\mathbf{r_i}) = [t(\mathbf{r_i}) + u(\mathbf{r_i})]\,\psi_\alpha(\mathbf{r_i}) = \epsilon_\alpha\psi_\alpha(\mathbf{r_i}).$$

As defined previously, for modelling a quantum dot we will equate $\hat{h}_i$ with the single-particle Hamiltonian of the harmonic oscillator. Then the energies

---

[1]We reserve Ψ as labelling for our exact wave function (eigen function, since there is no time-dependence). The Slater determinant is only an approximation of the exact solution.

ϵ_α are the so-called non-interacting single-particle energies, or unperturbed energies. The total energy is in this case the sum over all single-particle energies, if no two-body or more complicated many-body interactions are present.

We note again that the wave-function is antisymmetric with respect to an interchange of any two particles, as required by the Pauli principle. For an N-body Slater determinant we have thus (omitting the quantum numbers $\alpha, \ldots, \sigma$)

$$\Phi(\mathbf{r_1}, \mathbf{r_2}, \ldots, \mathbf{r_i}, \ldots, \mathbf{r_j}, \ldots, \mathbf{r_N}) = -\Phi(\mathbf{r_1}, \mathbf{r_2}, \ldots, \mathbf{r_j}, \ldots, \mathbf{r_i}, \ldots, \mathbf{r_N}).$$

5.3.3 Approximated energy of the system

Assume E_0 to be the ground state energy. According to the variational principle (given in eq. 5.11) we have

$$E_0 \le E[\Phi_T] = \int \Phi_T^* \hat{H} \Phi_T d\tau$$

where we have used the shorthand $d\tau = d\mathbf{r_1}, d\mathbf{r_2}, \ldots, d\mathbf{r_N}$, and where Φ_T is a trial function which we assume to be normalized

$$\int \Phi_T^* \Phi_T d\tau = 1.$$

In the Hartree-Fock method, correlations between electrons are not taken into account and the trial function is just the Slater determinant of eq. (5.17) which can be rewritten as

$$\Phi_T(\mathbf{r_1}, \mathbf{r_2}, \ldots, \mathbf{r_N}, \alpha, \beta, \ldots, \sigma) = \frac{1}{\sqrt{N!}} \sum_p (-)^p P \Psi_\alpha(\mathbf{r_1}) \Psi_\beta(\mathbf{r_2}) \ldots \Psi_\sigma(\mathbf{r_N}) = \sqrt{N!} \mathcal{A} \Phi_H$$

(5.18)

where we have introduced the antisymmetrization operator $\mathcal{A}$ defined by the summation over all possible permutations of 2 nucleons. It is defined as

$$\mathcal{A} = \frac{1}{N!} \sum_P (-)^p \hat{P},$$ (5.19)

with p standing for the number of permutations. We have introduced here the so-called Hartree function, defined by the simple product of all possible single-particle functions

$$\Phi_H(\mathbf{r_1}, \mathbf{r_2}, \ldots, \mathbf{r_N}, \alpha, \beta, \ldots, \sigma) = \Psi_\alpha(\mathbf{r_1}) \Psi_\beta(\mathbf{r_2}) \ldots \Psi_\sigma(\mathbf{r_N}). \quad (5.20)$$

Both $\hat{H}_0$ and $\hat{H}_1$ are invariant under all possible permutations of any two electrons and hence commute with $\mathcal{A}$

$$[\hat{H}_0, \hat{\mathcal{A}}] = [\hat{H}_1, \hat{\mathcal{A}}] = 0. \tag{5.21}$$

Furthermore, $\mathcal{A}$ satisfies

$$\mathcal{A}^2 = \mathcal{A} \tag{5.22}$$

since every permutation of the Slater determinant reproduces it.
The expectation value of $\hat{H}_0$

$$\langle \Phi_T | \hat{H}_0 | \Phi_T \rangle = \int \Phi_T^* \hat{H}_0 \Phi_T d\tau = N! \int \mathcal{A}\Phi_H^* \hat{H}_0 \mathcal{A}\Phi_H d\tau$$

$$= N! \int \Phi_H^* \hat{H}_0 \mathcal{A}^2 \Phi_H d\tau$$

$$= N! \int \Phi_H^* \hat{H}_0 \mathcal{A} \Phi_H d\tau$$

where we have used eq. (5.21) and (5.22). The next step is to replace the antisymmetrization operator by its definition in eq.(5.19) and to replace $\hat{H}_0$ with the sum of one-body operators as in eq.(5.16)

$$\int \Phi_T^* \hat{H}_0 \Phi_T d\tau = \sum_{i=1}^{N} \sum_{P} (-)^p \int \Phi_H^* \hat{h}_i \hat{P} \Phi_H d\tau.$$

The integral vanishes if two or more electrons are permuted in only one of the Hartree functions Φ_H because the individual single-particle wave functions are assumed orthogonal ($\langle \Psi_\alpha | \Psi_\beta \rangle = \delta_{\alpha\beta}$).
We obtain then

$$\int \Phi_T^* \hat{H}_0 \Phi_T d\tau = \sum_{i=1}^{N} \int \Phi_H^* \hat{h}_i \Phi_H d\tau.$$

The orthogonality of the single-particle functions allows us to further simplify the integral, and we arrive at the following expression for the expectation values of the sum of one-body Hamiltonians (i.e.the expectation value of the non-interacting single particle energies)

$$\int \Phi_T^* \hat{H}_0 \Phi_T d\tau = \sum_{\mu=1}^{N} \int \Psi_\mu^*(\mathbf{r}) \hat{h} \Psi_\mu(\mathbf{r}) d\mathbf{r} = \sum_{\mu=1}^{N} \langle \mu | h | \mu \rangle \tag{5.23}$$

Regarding the interaction part, the expectation value of the two-body Hamiltonian is obtained in a similar manner. We have

$$\langle \Phi_T | \hat{H}_1 | \Phi_T \rangle = \int \Phi_T^* \hat{H}_1 \Phi_T d\tau = N! \int \mathcal{A}\Phi_H^* \hat{H}_1 \mathcal{A}\Phi_H d\tau,$$

which reduces to

$$\int \Phi_T^* \hat{H}_1 \Phi_T d\tau = \sum_{i<j=2}^{N} \sum_P (-)^p \int \Phi_H^* V(r_{ij}) \hat{P} \Phi_H d\tau,$$

by following the same arguments as for the one-body Hamiltonian. Because of the dependence on the inter-electron distance r_{ij}, permutations of any two electrons no longer vanish.

$$\int \Phi_T^* \hat{H}_1 \Phi_T d\tau = \sum_{i<j=2}^{N} \int \Phi_H^* V(r_{ij}) \Phi_H d\tau - \int \Phi_H^* V(r_{ij}) P_{ij} \Phi_H d\tau$$

$$= \sum_{i<j=2}^{N} \int \Phi_H^* V(r_{ij})(1 - P_{ij}) \Phi_H d\tau,$$

where P_{ij} is the permutation operator that interchanges electron i and electron j. Again we use the assumption that the single-particle wave functions are orthogonal (as eigenvectors of an hermitian operator, the Hamiltonian), and we get

$$\int \Phi^* \hat{H}_1 \Phi d\tau = \frac{1}{2} \sum_{\mu=1}^{N} \sum_{\nu=1}^{N} \left[\int \Psi_\mu^*(\mathbf{r_i}) \Psi_\nu^*(\mathbf{r_j}) V(r_{ij}) \Psi_\mu(\mathbf{r_i}) \Psi_\nu(\mathbf{r_j}) d\mathbf{r_i} d\mathbf{r_j} \right] \quad (5.24)$$

$$-\frac{1}{2} \sum_{\mu=1}^{N} \sum_{\nu=1}^{N} \left[\int \Psi_\mu^*(\mathbf{r_i}) \Psi_\nu^*(\mathbf{r_j}) V(r_{ij}) \Psi_\mu(\mathbf{r_j}) \Psi_\nu(\mathbf{r_i}) d\mathbf{r_i} d\mathbf{r_j} \right] \quad (5.25)$$

The first term is the so-called direct term. It is frequently also called the Hartree term, while the second is due to the Pauli exclusion principle and is called the exchange term or just the Fock term. The factor $1/2$ is introduced because we now run over all pairs twice.

The last equation allows us to introduce soe further definitions. The single-particle wave functions $\Psi_\mu(\mathbf{r})$, defined by the quantum number μ and $\mathbf{r}$ (recall that $\mathbf{r}$ also includes spin degree) are defined as

$$\Psi_\alpha(\mathbf{r}) = \langle \mathbf{r} | \alpha \rangle$$

Since we will work in what is called the occupation number representation (or just second quantization) of quantum mechanical states and operators, we will not show the coordinate space dependence of various quantum mechanical objects.

We introduce the following shorthands for the above two integrals

$$\langle \mu\nu|V|\mu\nu \rangle = \int \Psi_\mu^*(\mathbf{r_i})\Psi_\nu^*(\mathbf{r_j})V(r_{ij})\Psi_\mu(\mathbf{r_i})\Psi_\nu(\mathbf{r_j})d\mathbf{r_i}d\mathbf{r_j}$$

and

$$\langle \mu\nu|V|\nu\mu \rangle = \int \Psi_\mu^*(\mathbf{r_i})\Psi_\nu^*(\mathbf{r_j})V(r_{ij})\Psi_\nu(\mathbf{r_i})\Psi_\mu(\mathbf{r_j})d\mathbf{r_i}d\mathbf{r_j}$$

Since the interaction is invariant under the interchange of two particles it means for example that we have

$$\langle \mu\nu|V|\mu\nu \rangle = \langle \nu\mu|V|\nu\mu \rangle,$$

or in the more general case

$$\langle \mu\nu|V|\sigma\tau \rangle = \langle \nu\mu|V|\tau\sigma \rangle.$$

The direct and exchange matrix elements can be brought together if we define the antisymmetrized matrix element

$$\langle \mu\nu|V|\mu\nu \rangle_{AS} = \langle \mu\nu|V|\mu\nu \rangle - \langle \mu\nu|V|\nu\mu \rangle,$$

or for a general matrix element

$$\langle \mu\nu|V|\sigma\tau \rangle_{AS} = \langle \mu\nu|V|\sigma\tau \rangle - \langle \mu\nu|V|\tau\sigma \rangle.$$

It has the symmetry property

$$\langle \mu\nu|V|\sigma\tau \rangle_{AS} = -\langle \mu\nu|V|\tau\sigma \rangle_{AS} = \langle \nu\mu|V|\sigma\tau \rangle_{AS}.$$

The antisymmetric matrix element is also hermitian, implying

$$\langle \mu\nu|V|\sigma\tau \rangle_{AS} = \langle \sigma\tau|V|\mu\nu \rangle_{AS}.$$

With these notations we write eq.(5.24) as

$$\langle \Phi_T|\hat{H}_1|\Phi_T \rangle = \int \Phi_T^* \hat{H}_1 \Phi_T d\tau = \frac{1}{2}\lambda^* \sum_{\mu=1}^N \sum_{\nu=1}^N \langle \mu\nu|V|\mu\nu \rangle_{AS}. \qquad (5.26)$$

Combining eqs.(5.23) and (5.26) we obtain the energy functional

$$E[\Phi_T] = \sum_{\mu=1}^N \langle \mu|h|\mu \rangle + \frac{1}{2}\lambda^* \sum_{\mu=1}^N \sum_{\nu=1}^N \langle \mu\nu|V|\mu\nu \rangle_{AS}. \qquad (5.27)$$

which we will use as our starting point for the Hartree-Fock calculations.

5.3.4   The restricted Hartree-Fock equations and their self-consistent solutions

Since it is based on a variational method and Lagrange multipliers (discussed in section 5.3.1), the Hartree-Fock technique also aims at minimizing the energy functional given in eq. 5.27. Nevertheless obtaining an eigenvalue problem to solve the eigenvalue problem is not straight forward when dealing with many interacting particles (as shown in 5.3.1) until we do a second approximation about the interacting potential.

Indeed the Coulomb repulsion induces a two-body interaction. As we show in the following, this leads to a system of coupled single-particle equations. A way to decouple those equations is to define an *effective potential*, which is an average of the Coulomb repulsion over all the electrons of the system. That is why the Hartree-Fock method is categorized as a *mean-field approximation* or also a *self-consistent field approximation* when refering to the iterative process of the method.

The following discussion only details the Restricted Hartree-Fock (RHF) method, where the quantum dot is modelled as a closed-shell system with all orbitals doubly occupied (electrons spin up and down). Open-shell systems, where some of the electrons are not paired, are not treated in this thesis, but can be handled by one of these other Hartree-Fock methods:

– Restricted open-shell Hartree-Fock (ROHF)

– Unrestricted Hartree-Fock (UHF)

[SAY SOMETHING about ROOTHAN equations]
The Roothaan equations are a representation of the Hartree-Fock equation in a <u>non-orthonormal</u> basis set which can be of Gaussian-type or Slater-type. It applies to closed-shell systems where all orbitals are doubly occupied. This is generally called Restricted Hartree-Fock theory. The method was developed independently by Clemens C. J. Roothaan and George G. Hall in 1951, and is thus sometimes called the Roothaan-Hall equations. The Roothaan equations can be written in a form resembling generalized eigenvalue problem, although they are not a standard eigenvalue problem because they are nonlinear:

$$\mathbf{FC} = \mathbf{SC}\epsilon$$

where F is the so-called Fock matrix (which depends on the coefficients C due to electron-electron interactions), C is a matrix of coefficients, S is the overlap matrix of the basis functions, and ϵ is the (diagonal, by convention) matrix of orbital energies. In the case of an orthonormalised basis set the overlap matrix, S, reduces to the identity matrix.

[DIFFERENT IMPLEMENTATION OF THE HARTREE-FOCK METHOD: 2 techniques to do that (cf.Morten slides in FYS4410): either vary the spatial part of the single particle wave functions, or expand each single particle wave functions in a given basis (i.e. the HO basis set) and vary the coefficients of those single particle wf. In the following, we use the latter technique, which is the more common (industrial) way to apply Hartree-Fock.]

One technique for solving this problem starts by expanding each single-particle eigenvector Ψ_i in terms of any convenient complete set of single-particle states $|\alpha\rangle$:

$$\Psi_i = |i\rangle = \sum_\alpha c_i^\alpha |\alpha\rangle. \tag{5.28}$$

In our case, the complete set of single-particle states $|\alpha\rangle$ corresponds to the harmonic oscillator states. While the expansion (5.28) in general involves an infinite number of terms, we always truncate it in approximation procedures, so that we shall assume here that (5.28) is a finite sum [50] in the subspace of dimension K.

$$\Psi_i = |i\rangle = \sum_\alpha^K c_i^\alpha |\alpha\rangle. \tag{5.29}$$

Introducing the expansion (5.29) in the expectation value of $\hat{H}$ (eq. 5.27), we can write

$$E[\Phi] = \langle\Phi|\hat{H}_0|\Phi\rangle + \langle\Phi|\hat{H}_1|\Phi\rangle \tag{5.30}$$

$$= \sum_{i=1}^N \langle i|h|i\rangle + \frac{1}{2}\lambda^* \sum_{i=1}^N \sum_{j=1}^N \langle ij|V|ij\rangle_{AS} \tag{5.31}$$

$$= \sum_{i=1}^N \sum_{\alpha\gamma}^K C_i^{\alpha*} C_i^\gamma \langle\alpha|h|\gamma\rangle + \frac{1}{2}\lambda^* \sum_{i,j=1}^N \sum_{\alpha\beta\gamma\delta}^K C_i^{\alpha*} C_j^{\beta*} C_i^\gamma C_j^\delta \langle\alpha\beta|V|\gamma\delta\rangle_{AS}. \tag{5.32}$$

the objective is of course to minimize the energy functional in eq. 5.30 with respect to some constraints that insure the orthonormality of the single-particle eigenvectors. For that purpose we introduce the ϵ_i as Lagrange multipliers to insure the constraints of orthonormality, meaning for any particle

i and j

$$\langle i|j \rangle = \delta_{ij}$$

$$\sum_{\alpha\beta}^{K} C_i^{\alpha*} C_j^{\beta} \underbrace{\langle \alpha|\beta \rangle}_{\delta_{\alpha\beta}} = \delta_{ij} \tag{5.33}$$

$$\sum_{\alpha}^{K} C_i^{\alpha*} C_j^{\alpha} = \delta_{ij} \tag{5.34}$$

Then a variatonal analysis implies minimizing the Lagrangian Λ

$$\Lambda = \Lambda(C_1^{\alpha}, C_2^{\alpha}, \ldots, C_N^{\alpha}, \epsilon_1, \epsilon_2, \ldots, \epsilon_N), \tag{5.35}$$

$$= E[\Phi] - \sum_{i=1}^{N} \epsilon_i \left(\sum_{\alpha}^{K} C_i^{\alpha*} C_i^{\alpha} \right), \tag{5.36}$$

with respect to the coefficient $C_i^{\alpha*}$ (or C_i^{α}).

The variational equation as defined in 5.6 leads to take the derivative of (5.35) with respect to $C_i^{\alpha*}$ and to set it to zero

$$\frac{d}{dC_i^{\alpha*}} \left[\Lambda(C_1^{\alpha}, C_2^{\alpha}, \ldots, C_N^{\alpha}, \epsilon_1, \epsilon_2, \ldots, \epsilon_N) \right] = 0 \quad \forall\, i \in \mathbb{N}^*$$

$$\frac{d}{dC_i^{\alpha*}} \left[E[\Phi] - \sum_{i=1}^{N} \epsilon_i \sum_{\alpha}^{K} C_i^{\alpha*} C_i^{\alpha} \right] = 0 \quad \forall\, i \in \mathbb{N}^*.$$

Remembering that C_i^{α} and $C_i^{\alpha*}$ can be treated as independent, we arrive at the Hartree-Fock equations (one equation for each particle i in its state $|\alpha\rangle$)

$$\sum_{\gamma}^{K} \langle \alpha|h|\gamma \rangle\, C_i^{\gamma} + \lambda^* \sum_{j=1}^{N} \sum_{\beta\gamma\delta}^{K} C_j^{\beta*} \langle \alpha\beta|V|\gamma\delta \rangle_{AS}\, C_i^{\gamma}\, C_j^{\delta} = \epsilon_i\, C_i^{\alpha} \quad \forall\, i \in \mathbb{N}^* \tag{5.37}$$

The Hartree-Fock equations in (5.37) may be rewritten as

$$\sum_{\gamma}^{K} \langle \alpha|h|\gamma \rangle\, C_i^{\gamma} + \lambda^* \sum_{\gamma}^{K} \left[\sum_{j=1}^{N} \sum_{\beta\delta}^{K} C_j^{\beta*} \langle \alpha\beta|V|\gamma\delta \rangle_{AS}\, C_j^{\delta} \right] C_i^{\gamma} = \epsilon_i\, C_i^{\alpha} \quad \forall\, i \in \mathbb{N}^*$$

$$\sum_{\gamma}^{K} \mathcal{O}_{\alpha\gamma}\, C_i^{\gamma} = \epsilon_i\, C_i^{\alpha} \quad \forall\, i \in \mathbb{N}^* \tag{5.38}$$

from where we notice that eq.(5.37) is a system of non-linear equations in the C_i^α, $C_i^{\alpha*}$, since $\mathcal{O}_{\alpha\gamma}$ depends itself on the unknowns, which may be solved by an iterative procedure.

The iterative (self-consistant) procedure may be derived as follows. Let us define an *effective Coulomb interaction potential U* as

$$\langle\alpha|U|\gamma\rangle \equiv \lambda^* \sum_{j=1}^{N} \sum_{\beta\delta} C_j^{\beta*} \langle\alpha\beta|V|\gamma\delta\rangle_{AS}\, C_j^\delta \qquad (5.39)$$

and calculate these matrix elements with initial values for C_i^α, say δ_i^α. When we substitute the result in eq.(5.37), we get a system of linear equations in the C_i^α; this we can now solve in the standard way. If we started with a set of K states $|\alpha\rangle$, the vectors C_i^α are K-dimensional and orthogonal, and so obey

$$\sum_{\alpha}^{K} C_i^{\alpha*} C_j^\alpha = \delta_{ij}.$$

There are thus K independent vector solutions of the linearised version of eq.(5.37),

$$\sum_{\gamma}^{K} \left[\langle\alpha|h|\gamma\rangle + \langle\alpha|U|\gamma\rangle\right] C_i^\gamma = \epsilon_i\, C_i^\alpha.$$

Among those solutions we select those for the n lowest eigenvalues ϵ_i and substitute them back into (5.39); this provides the starting point for the next iteration. The process is continued until self-consistency is reached, or in other words until the C_i^α converge within a certain approximation [50].

The Hartree-Fock equations in (5.37) may again be rewritten as

$$\sum_{\gamma}^{K} \langle\alpha|h|\gamma\rangle\, C_i^\gamma + \lambda^* \sum_{\gamma}^{K} \left[\sum_{j=1}^{N} \sum_{\beta\delta}^{K} C_j^{\beta*} \langle\alpha\beta|V|\gamma\delta\rangle_{AS}\, C_j^\gamma\, C_j^\delta \right] C_i^\gamma = \epsilon_i\, C_i^\alpha \quad \forall\, i \in \mathbb{N}^*$$

$$\sum_{\gamma}^{K} \left[t_{\alpha\gamma} + \lambda^* \sum_{j=1}^{N} \sum_{\gamma,\delta=1}^{K} V_{\alpha\beta\gamma\delta}\, C_j^{\beta*}\, C_j^\delta \right] C_i^\gamma = \epsilon_i\, C_i^\alpha \quad \forall\, i \in \mathbb{N}^*$$
$$(5.40)$$

where the two-body interaction matrix element $V_{\alpha\beta\gamma\delta}$ can be computed in advance

$$V_{\alpha\beta\gamma\delta}(ij) = \langle\alpha\beta|V(ij)|\gamma\delta\rangle_{AS}$$

as well as the one-body piece $t_{\alpha\gamma}(i)$

$$\sum_{\gamma}^{K} t_{\alpha\gamma}(i) = \sum_{\gamma}^{K} \langle\alpha|h(i)|\gamma\rangle = \epsilon_{HO}^{\alpha}$$

where ϵ_{HO}^{α} are the energy eigenvalues of the one-body harmonic oscillator in state $|\alpha\rangle$ (then solution of the eigenproblem: $h_{HO}|\alpha\rangle = \epsilon_{HO}^{\alpha}|\alpha\rangle$).

5.3.5 Computational efficiency of the Hartree-Fock method

"Time complexity" and "space complexity" (memory requirements)

try to reproduce Simen's derivation when looking at the accuracy of the method [PhD p.25 [4]].

5.4 Corrections to the HF energy: perturbation theory

5.4.1 2nd and 3rd order time-independent degenerate perturbation theory corrections

detailled in [52, 53] about second order and third order expressions.

5.4.2 Occupation number formalism

detailled in [53], Hamiltonian formalism in [OpenFCI paper of Simen] and [chap.2 from Morten lectures] and [http://www.iue.tuwien.ac.at/phd/pourfath/node109.html]

When we start developing the expression of an excited state of the unperturbed Hamiltonian as given from the perturbation theory, it becomes really complicated to write the combinations of Slater determinants in terms of permutations of occupied and unoccupied single particle orbitals.

Historically, quantum physics first dealt only with the quantization of the motion of particles, leaving the electromagnetic field classical (Schrödinger, Heisenberg and Dirac, 1925-26). Later also the electromagnetic field was quantized (Dirac, 1927), and even the particles themselves got represented by quantized fields (Jordan and Wigner, 1927), resulting in the development of quantum electrodynamics and quantum field theory in general. By convention, the original form of quantum mechanics is denoted first quantization, while quantum field theory is formulated in the language of occupation number formalism, also known as second quantization.

As we will show, second quantization greatly simplifies the discussion of many interacting particles. This approach merely reformulates the original

Schrödinger equation. Nevertheless, it has the advantage that in second quantization operators incorporate the statistics, which contrasts with the more cumbersome approach of using symmetrized or anti-symmetrized products of single-particle wave functions. In the second quantization formalism a quantum mechanical basis is used that describes the number of particles occupying each state in a complete set of single-particle states. For this purpose the time-independent abstract state vectors for an N-particle system are introduced

$$|n_1, n_2, \ldots\rangle, \quad where \quad \sum_j n_j = N. \tag{5.41}$$

The notation means that there are n_1 particles in the state 1, n_2 particles in the state 2, and so forth. It is therefore natural to define occupation number operators $\hat{n}_j$ which have the basis states $|n_j\rangle$ as eigenstates, and have the number n_j of particles occupying the state j as eigenvalues $\hat{n}_j|n_j\rangle = n_j|n_j\rangle$. For fermions (such as the electrons of our quantum dot) n_j can be 0 or 1, while for Bosons it can be any non-negative number.

5.5   Variational Monte-Carlo method

see vmx.tex given by Morten [email 28/05/2009]

5.6   Full Configuration Interaction (Exact or Large Scale Diagonalization) method

A configuration interaction wave function is a multiple-determinant wave function. This can be constructed by starting with the HF wave function and making new determinants by promoting electrons from the occupied to unoccupied orbitals. Configuration interaction calculations can be very accurate, but the cost in CPU time is very high (N^8 time complexity or worse).

Configuration interaction calculations are classified by the number of excitations used to make each determinnat. If only one electron has been moved for each determinant, it is called a configuration interaction single-excitation (CIS) calculation. CIS calculations give an approximation to the excited states of a molecule, but do not change the ground-state energy. Single and double excitation (CISD) calculations yield a ground state energy that has been corrected for correlation. Triple-excitation (CISDT) and quadruple-

excitation (CISDTQ) calculations are done only when very-high-accuracy resuts are desired.

The configuration interaction calculation with all possible excitations is called a full CI. The full CI calculation using an infinitely large basis set will give an exact quantum mechanical result. However, full CI calculations are very rarely done due to the immense amount of computer power required.

[Some more info about the reference used (HF or Gaussian) in input in Google book on computational chemistry.]

[also in Simen thesis: CI+effective interaction in paper 1]

5.6.1 Effective Interaction

5.7 Corrections to the HF energy: perturbation theory

5.8 Time-dependent Hartree-Fock Theory

paper from Moan on How to solve a Time-dependent Schro. eq. using "Splitting methods" (weekly meeting 10/09/2008)

5.9 Comparison with Variational Monte Carlo???

info about that in the thesis from Rontani

may include a comparison as done last semester between DFT and HF!!!!

Chapter 6

Implementation and Results

TEST to cite a class: class `CoulombMatrix`

```
% Place nodes
\node [block] (init) {Initialize:\\
Set $\mathbb{R}$, $\alpha$ and $\Psi_{T-\alpha}(\mathbb{R})$};
\node [block, below of=init] (suggestMove) {Suggest a move};%:\\ $\mathbb{x}^{trial}_p
\node [block, below of=suggestMove] (evaluateAcceptance) {Compute acceptance ratio};%:
```

[use code here to generate DECISION TREES, same guy who made timer.hpp: http://oldmill.uchicago.edu/ wilder/Code/pst/]

Give a list of states, non-ordered, then ordered an explain why.

Detail constraint on momentum/spin conservation on the implementation

6.1 Code Implementation in the energy basis

[DESCRIBES THE IMPLEMENTATION AS A LOGICAL REPRESENTATION OF THE BLACK BOX OF THE HF METHOD]

The main program processes a textual configuration file (*parameters.inp*) with problem parameters (size of the closed shell system, dimension of the problem, interaction strength,...) before proceeding with the Hartree-Fock algorithm. While running the executable, the Hartree-Fock approximation of the total energy is computed in a self-consistent way and finally printed out to screen.

The code is organized in different classes to allow generalization of the problem, and more particularly the possibilities to compute the Hartree-Fock approximation of the total energy using different methods (analytical expression of the Coulomb interaction or numerical integration in different basis set using the Numerov's algorithm instead of solving an eigenvalue
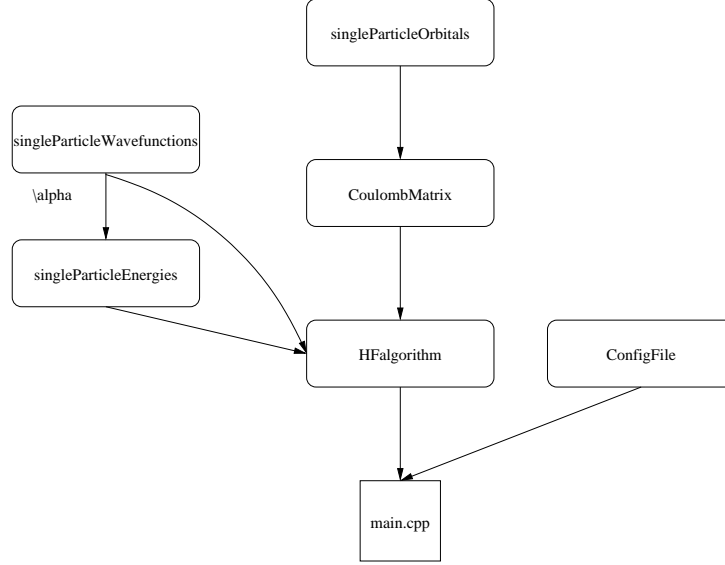
Figure 6.1: Diagram of the code implementation

problem) and for different forms of the confining potential, in two and three dimensions.

; ;

Figure [6.1] tries to summarize the code implementation in a diagram.

The current version only consider closed-shell systems where particles are trapped within an isotropic harmonic oscillator potential. Given the maximum energy level R, the class *singleParticelOrbitals* generates all single particle states and build a table of states with their respective quantum numbers ($|\alpha\rangle \rightarrow |n, ml, ms\rangle$) in both 2D and 3D. The class *CoulombMatrix* generates and stores a matrix of the 2-body Coulomb interaction computing its analytical expression [46] [54] in two dimension only.

$$V_{\alpha\beta\gamma\delta} = \langle\alpha\beta|V_{ij}|\gamma\delta\rangle_{as}.$$

The classes *singleParticleWavefunctions* and *singleParticleEnergies* are assumed to provide respectively multiple choices of basis set ($|\alpha\rangle \rightarrow \varphi_\alpha(r, \theta, \phi)$) and their corresponding single particle energies ($|\alpha\rangle \rightarrow \epsilon_\alpha = \langle\alpha|\hat{h}|\alpha\rangle$). Since the Coulomb matrix elements are computed in 2D from an analytical expression obtained in the harmonic oscillator basis set, no numerical integration are required in the current version of the code. This is the reason why no explicit basis, neither numerical integration methods have been implemented yet. The single particle energies for non-interacting particles have also simple analytical forms in the harmonic oscillator basis

($\epsilon_\alpha^{HO} = 2n + |m_l|$ in 2D). Then the classes $singleParticleWavefunctions$ and $singleParticleEnergies$ are really simple now, but have been created for future generalization of the code.

The class $HFalgorithm$ solves the Hartree-Fock equations by solving an eigenvalue problem. This eigenvalue problem comes from the expansion of the single particle wave functions in the harmonic oscillator basis set and from the initialization of an effective potential initially computed thanks to a guess of the single particle wave functions and the pre-computed Coulomb matrix elements. This class also implements an iterative procedure, where the solution of the eigenvalue problem are injected back into the computation of the effective potential. This new effective potential is then used to solve a new eigenvalue problem, giving rise to a new set of single particle wavefunctions and a lower energy of the system. The process is continued until self-consistency is reached.

The main file reads the paramters of the problem from file and simply build the objects of the classes described earlier one after the other in order to define, to initialize and to solve the problem. An example of the basic configuration file is shown below.

```
##############################################################################
#                                                                            #
# *** parameters.inp contains input parameters for the simulation of    #
#     a quantum dot using closed-shell Hartree-Fock  ***                #
#                                                                            #
##############################################################################


###############################
# --- model space parameters ---

dimension = 2    # [dim or d] 2D or 3D
R_basis = 2      # [Rb or b] maximum shell number for the HO basis
                     set (ex. R=2n+|m| in 2D)
R_fermi = 0      # [Rf or f] Fermi level defining #electrons in the
                     closed shell system
includeCoulombInteractions = yes # [coulomb or c] Switch ON/OFF the
                                     Coulomb piece


###############################
# --- interaction parameters ---
lambda = 1.0     # [lambda or l] strength of the interaction

###############################
# --- Hartree-Fock parameters ---
epsilon = 1e-16; # [epsilon or e] precision used for self-consistency
                   of the total energy

kappa = 1.0;     # double btw [0,1] for optimisation of the convergence,
                   tests show that kappa=1 is the fastest anyway


###############################
# --- computational parameters ---
```

```
readFromOpenFCI = yes # [openFCI or r] read single element for Coulomb
                             piece from OpenFCI instead of analytical
                       expression of Rontani
kinetic        = no  # [kinetic or kin] use the kinetic energy of the
                       HO as single particle H, otherwise, the full HO
                       hamiltonian is used
computePTcorrection = no # Boolean to compute or not Perturbation Theory
                            correction to the HF energy
save_states          = no # [] write table of quantum states

save_EigValPb        = yes# [] write the Blocks to diagonalize and the
                                    eigenvalues to file

# name of the ouput file that stores eigenValues over iterations
filenameLogEigVal    = outputs/logEigenValues.txt

# name of the ouput file that stores Blocks to "occupied" diagonalize
over iterations
filenameLogBlock     = outputs/logBlockDiag.txt

# name of the ouput file that stores eigenVectors to "occupied" diagonalize
over iterations
filenameLogEigVec    = outputs/logEigenVectors.txt

perturbationTheory   = yes # compute the Perturbation theory up to 3rd order
                                with the interaction expressed in the HO basis
HF_PT_correction     = yes # compute the 2nd and 3rd order pertubation theory
                                corrections terms to the HF ground state energy


###############################

You can either change here the input parameters before running the
executable or you can overwrite them using command lines:
ex.: ./project dim 2  Rf 1 Rb 5 lambda 1.4 pt 1 HF_PT 1
     will run the Hartree-Fock code in 2D, for a closed-shell system
     up to n=1, expanded in the HO basis up to shell #5,
     using a confinement strength equal to 1.4,
     computing HF correction up to 3rd order to the HF energy,
     and independently of HF, computing the corresponding perturbation
     theory in the HO basis.

or simply:
ex.: ./project d 2 f 1 b 5 l 1.4 o output.m

Other options/shortcuts maybe not listed above [OPTION] [VALUES]:
- [d OR dim] [2 or 3]
- [b OR Rb OR R_basis] [positive integer]
- [f OR Rf OR Rfermi] [positive integer]
- [lambda OR l] [positive double]
- [epsilon OR e] [positive double]
- [coulomb OR cp] [boolean]
- [openFCI OR readCI OR r] [boolean]
- [perturbationTheory OR pt] [boolean]
- [HF_PT_correction OR HF_PT] [boolean]
- [logInfos OR log] [boolean]
```

As an example, table 6.1 shows a different ground state Hartree-Fock energies (in units of $\hbar\omega_0$) when varying the parameters *dimension*, *R*, *lambda* and running the executable each time.

	2D			3D		
R	# e^-	$\lambda = 1$	$\lambda = 2$	# e^-	$\lambda = 1$	$\lambda = 2$
0	2	3.25331	4.50663	2		
1	6	22.21981	34.43963	8		
2	12	73.76555	119.53110	20		
3	20	177.96330	295.92660	40		
4	30	357.54370	605.08739	70		
5	42	637.55964	1093.11930	112		

Table 6.1: Hartree-Fock approximations of the ground state energy of the quantum dot obtained for different sets of input parameters in two and three dimensions.

Table **??** compares the ground state energies reported in [???] with my Hartree-fock approximation. [NOT FOUND A REFERENCE YET !!]

The code does not support parallel computation yet. This could be useful when solving the eigenvalue problem or computing numerical integrations, but the code is already fast enough to produce results in a few second or minutes for reasonnably large systems ($R \leq 4$).

6.1.1   The Hilbert space

In this part, description of the way the basis set is build. Recall this is done on a closed shell system. Describe the tables of states in the basis set with their respective quantum numbers (in 2D and 3D), as wel las the table of "hole" states for the states occupied by a particle. Describe the table of states-couple, which is used in the generation of the Coulomb interaction.

Also describe the function that re-order the basis set within blocks of common angular momentum and spin. the reason for it is given later in the Hartree-Fock algo with consideration of parity invariance and when it comes to solve the eigenvalue problem, this re-ordering leads to a block diagonal matrix to diagonalize, which can then be split to several smaller matrices. This is much more efficient when it comes to solve the eigenvalue problem.

6.1.2   The Coulomb interaction

describe what we are building here and how (Analytical expression described in [54, 55, 56]).

6.1.3   The energy basis

analytical energies of the "single-states" in the Hibert space. Explain that this class simply computes the HO energies for each states of the basis set analytically. In the perspective of a more general problem with a confining potential different from the HO potential, these energies would be computed using numerical integration. That's why it is linked to a class of wave functions in their explicit form (including Laguerre polynomials for example in the case of the HO basis set).

6.1.4   The Hartree-fock algorithm

– Don't forget to mention **parity**:consider it liek one more quantum number, since ml should be conserved by the hamiltonian, if matrix organized by groups of states with identical ml, we should observe that his matrix is block diagonal, then reducing the eigenvalue problem to several (much smaller) eigenvalue problems.

– **Householder method** for tridiagonalization the $\tilde{A}\ddot{y}$atrix and **tqli()** to diagonalise the tridiagonal matrix obtained

details the link between this class, the algorithm described in 5.3.4 and how it calls oher part of the code described previoulsy (call to the basis set, the quantum numbers of each state in the set, the "hole" states, call to the Coulomb matrix elements).

explains that this class just performs the job done in one iteration of the iterative procedure, and that it can also check if the self-consistency is achieved or not.

Explain finally that the loop over iterations is done in the "main" class. This class is really simple, just

– defining the objects one after the others: the basis set, the Coulomb matrix, the Hartree-fock equations

– performing the loop over iteration calling for functions of the Hartree-Fock class to solve the eigenvalue problem and update the effective potential

– write to log the input/output data

– compute the duration of each part of the simulation

6.2 Numerical Analysis

6.2.1 Comparison with analytical results (TAUT, Espen with B fiedl, Simen)

2-electrons QD with interactions solved anaytically by TAUT. Write a sub-chapter in the theoretical background on QD!!!!

6.2.2 Comparison with other numerical calculations (VMC, DFT, Large Scale diag from Simen exact for 2 electrons)

References: Rune, Simen Kvaal, ... Fidn reference for Hartree-Fock Calculation of QD too !!!!!!! IMPORTANT !!! (VMC, DFT, Large Scale diag from Simen exact for 2 electrons)

6.2.3 Study of the convergence behaviour

speed (stability) and accuracy with respect to the arbitrary size of the basis of HO wf (discussion with Simen Kvaal 05/09/2008)

vendredi 5 septembre 2008 Discussion with Simen Kvaal: Reliability of my simulator??? 1. TO CHECK IF MY SIMULATOR OBTAINS GOOD RESULTS = compare to references

* check with Morten if any analytical solution of Hartree-Fock method for QD exists?? * Checks my results with references of numerical calculations

2. TO CHECK IF THE HF CODE WORKS

* test this interaction V(r12)=const/r12, there is an analytical solution of that. * test V(r12)=const=K, then V(rij)=KâĞŠ Îč V(rij) = N (N-1) K (trivial example, maybe too trivial since it may not show some error in the HF code) * finally check V(r12)=a.r12Âš+b

3. TO CHECK IF MY SIMULATOR IS CONVERGING PROPERLY (fast enough, with a sufficiently big basis of HO wave functions) Necessaire MAIS PAS SUFFISANT !!!!!

* basis made of HO wave functions=$\Phi_{nlm}|2n+|l|R$ for 3D case * R reprensents a given energy level composed of a lot of degenerate states * calculate the probability to be at a given energy level, probability: ÏĽ(R) o at a given energy level, a given R, and the set of wf at this level is: $\Phi_{nlm}|2n+|l| = R$ o then $(R) = \sum |\Phi_{nlm}|\Psi_j|^2$ with j such that $2n + |l| = R$ o plot log[ÏĽ(R)] as a function of log[R] o should observe ecponential convergence with Hartree-Fock (as Simen has seen during his summer course in august 2008) o if you see noise ($log[(R)] = 10^{(}-16))$, then you achieved the numerical precision of the machine o you can also plot: $\hat{T}$E(R)=E(R)-E(RâĹđ)

6.3   Toward a more realistic model of a colloidal QD

6.3.1   Impact of some defect on the surface of the quantum dot

Some defect might obviously change the potential energy from a spherical HO potentialto something else: ???

Will this lead to a Quantum chaos = some really strange/no symmetric eigenvalues???

This could be shown by studying the distribution of $\Delta E = E_{n+1} - E_n$ and see if we get the nice decreasing exponential (eigenstate not varying much from eachother) or a pseudo-gaussian characteristic from the chaotic behaviour???

Discussion at the Weekly Journal on the 11/09/08 by Simen Kvaal.

Might consider looking at the Green's function to solve such chaotic system, or at least approximation of the Green's function.

6.3.2   Impact of the environment on the system

New model for the external field applied: will a dipole or quadrupole field be a better approximation for the IR/UV radiations?

Is the coating and the acquous environment having any effect on the potential energy? What could be a better model of the potential?

Chapter 7

Computational Results and Analysis

7.1 Validation of the simulator

7.2 Validation of the model

Kouwenhoven: non-interacting particles display Fock-Darwin spectrum. For 2 electrons, the closed shell model (constant interaction model) breaks at $B = 26\ T$ (for typical values of GaAs). should reproduce those plots.. Numerical calculations shows that, without neglecting the electron interactions, the state transition occurs at a much loweer value $B \simeq 10\ T$. Should reproduce this with OpenFCI

7.2.1 Coulomb matrix generation

7.2.2 Non-interacting particles

7.3 Study of the Hartree-Fock Algorithm as a function of the size of the basis set

Hartree-Fock approximation to the ground state energies E_0^{HF} as a function of the size of the basis set R, for 3 differentes values of the confinement strenght $\lambda = 0.5, 1$ or 2.

Figure (7.1) presents the results of the simulator, providing the Hartree-Fock approximation to the ground state energy of a two-particle quantum dot where the charge carriers are confined with a dimensionless confinement strength $\lambda = 1$. In two-dimension, the exact ground state energy of such a
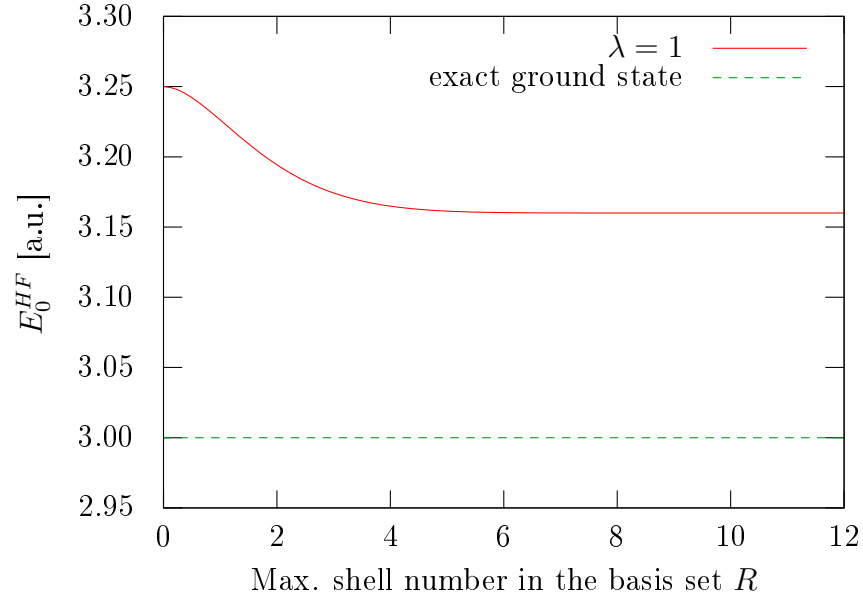
Figure 7.1: Hartree-Fock approximation to the ground state energy of a two-particle quantum dot, with a confinement strength $\lambda = 1$

system is known to be equal to $E_0 = 3$ in units of $\hbar\omega$ as shown in chapter 4. Therefore we see easily that Hartree-Fock provides a rough approximation to the exact energy with a difference of 5.33%.

7.4   Comparison: Hartree-Fock, Perturbation theory, VMC, FCI

shows breaking of perturbation theory much before Hartree-Fock when increasing the confinement strength.

shows breaking of HF compared to VMC and FCI as λ increases.

table of accuracy between the *ab-initio* methods for different values of λ. When $\lambda = 1$, can also compare to exact solution for two particles.

table with duration/complexity/model size achievable (nb.electrons) of the simulations for VMC/HF/PT/FCI and produce Spider chart to visually compare the methods.
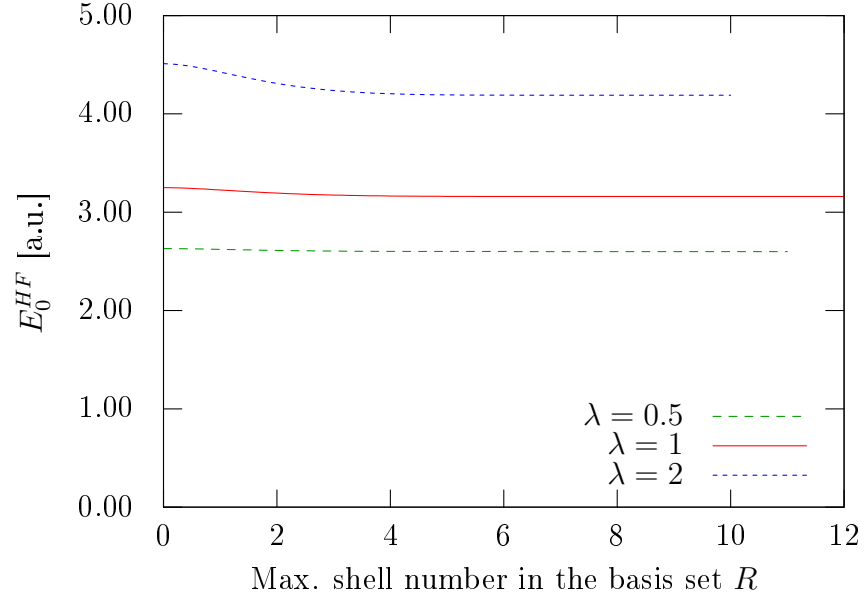
Figure 7.2: Hartree-Fock approximation to the ground state energy of a two-particle quantum dot, for different values of the confinement strength $\lambda = 0.5, 1$ or 2
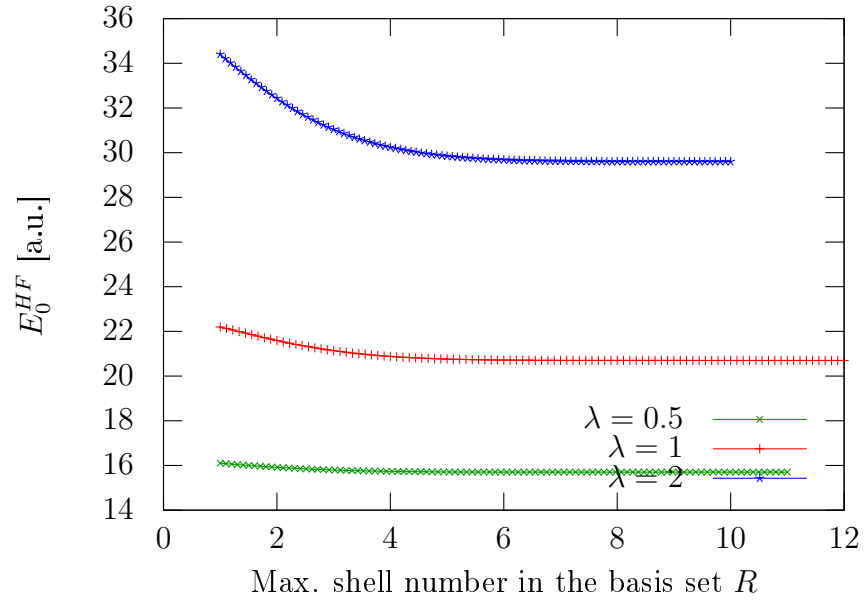

Figure 7.3: Hartree-Fock approximation to the ground state energy of a six-particle quantum dot, for different values of the confinement strength $\lambda = 0.5, 1$ or 2

Figure 7.4: Hartree-Fock approximation to the ground state energy of a twelve-particle quantum dot, for different values of the confinement strength $\lambda = 0.5, 1$ or 2
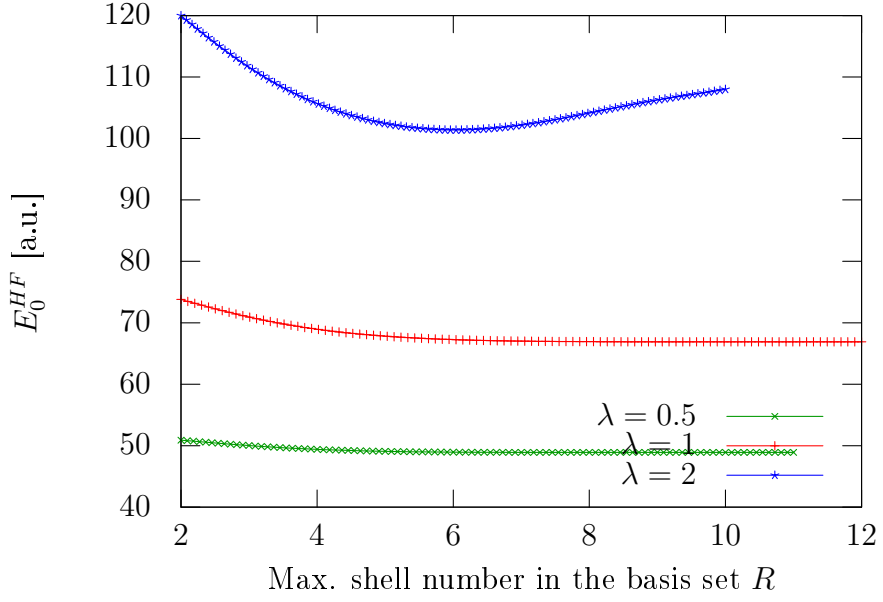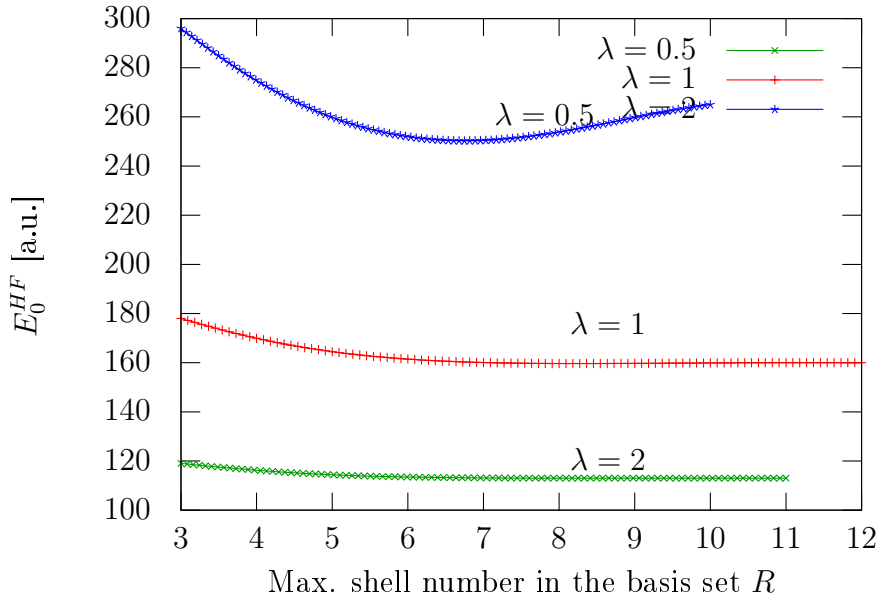

Figure 7.5: Hartree-Fock approximation to the ground state energy of a twenty-particle quantum dot, for different values of the confinement strength $\lambda = 0.5, 1$ or 2

7.5 Breaking of the closed-shell model study

Using OpenFCI, shows for 6 particles different ground state energies corresponding to different electronic structures. For 6 electrons, the closed shell system might not always be the optimal electron configuration as a function of the magnetic field.

note 7/06/2009 + test tin Simen/bin notes 19/05

Chapter 8

Conclusion

[critical discussion should lead to reflections, and reflections should lead to perspectives]

8.0.1   Findings + critical discussion of the results

Summary of subject, methods, results Be critical !!!!

 – what are the limitations of HF according to the strength of the confinement wrt other methods? Compare all methods to some theoretical/reference results.

   – accuracy wrt other methods for different the size of the system?

   – simulation duration (compare the limits of each method for a given system, and compare the size of the biggest system achievable by each method-> other method like **DFT** might be of interest to study huge system in a reasonnable amount of time)?

   – Are HF results accurate enough for the confinement (B field) in use today in laboratories for confining electrons in a quantum dot?

 – what are the improvements when using the HF basis set as input of VMC or CI? Does it really help (accuracy and duration improvements)?

 – I did it both in 2D and 3D (Waltersson 2007 [[57]] just in 2D), but not easy to compare since he didnt' include results for closed shell systems

8.0.2   Perspectives for future works

 – Rontani p.85 wrote a paper on the range of validity of different theoretical scheme and show a strong **impact of the dimensionality** of

the QD. Shows that 3D scheme are more adequate to describe real QD. [could lead to a study VMC from Rune, my Hf, CI from Espen to see how dimensionality affect the results for the different methods]

- not done in 3D yet since the Coulomb matrix expression was based on an analytical formula in 2D only, could improve it by doing numerical computation of the Coulomb Matrix elements and that will also allow to generalize to other confining potential than just the HO potential, maybe closer to more realistic systems (ex.: how to simulate the environment when we want to model colloidal QD)

- How the complexity increases with the size of the system (= with the nb. of electrons)? = DIMENSIONALITY (binomial M N en bas, avec M nb of state possible, N the nb. of particle) Cf: ComphPhys course + Simen ("curse of Dimensionality")

- HOW fast HF converges wrt other ab initio methods? It is possible to explicitely give the convergence rate?

- in order to make some visualization of the QD, plot density probability, BUT, since HF is based on effective potential, sphericcaly symm., we are not able to see much (I though I could see the point like electron by fixing one), but it might be possible to see some quantum effect if some regions are prohibited (we might see some rings)

Appendix A

Quantum Mechanics

A.1   The Quantum Mechanical Harmonic Oscillator

One of the very useful models in quantum mechanics is the harmonic oscillator. This model provides the basis for discussing any system fluctuating by small amounts near a configuration of stable equilibrium [Shankar]. It is the basis for extremely diverse many-body calculations in nuclear physics, quantum chemistry and quantum dot calculations in solid state physics. For completness, let's begin with a review of of the harmonic oscillator in 1D.

A.1.1   Single Harmonic Oscillator without spin in 1D

[J.E. HOUSE] In one-dimension, a spinless particle trapped in a harmonic oscillator potential well written as $\frac{1}{2}m\omega^2 x^2$ has Hamiltonian:

$$H_{\text{HO}} = -\frac{\hbar^2}{2m}\frac{\partial^2}{\partial x^2} + \frac{1}{2}m\omega^2 x^2, \tag{A.1}$$

The Schrodinger equation reads $\hat{H}\psi = E\psi$ where E stands for the eigenenergy and ψ its corresponding eigenvector. With the hamiltonian above, the Schrodinger equation becomes:

$$H_{\text{HO}}\psi(x) = E\psi(x)$$
$$\left(-\frac{\hbar^2}{2m}\frac{\partial^2}{\partial x^2} + \frac{1}{2}m\omega^2 x^2\right)\psi(x) = E\psi(x)$$

and can be simplified to the following non-linear differential equation:

$$\frac{\partial^2\psi(x)}{\partial x^2} = -\left(\frac{2mE}{\hbar^2} - \frac{m^2\omega^2}{\hbar^2}x^2\right)\psi(x) \tag{A.2}$$

To solve such an equation, let's assume a solution on the form: $\psi(x) = ce^{-bx^2}$ where $b, c \in \mathbb{R}$.

Then the 1st and 2nd derivatives of the wave function reads:

$$\frac{\partial \psi(x)}{\partial x} = -2bcxe^{-bx^2} = -2bx\psi(x)$$

$$\frac{\partial^2 \psi(x)}{\partial x^2} = -(2b - 4b^2x^2)\psi(x) \tag{A.3}$$

By comparing eqn.(refeq:nonlinearEqDiff) and (A.3), it comes that $b = \frac{m\omega}{2\hbar}$ and $E = \frac{\hbar\omega}{2}$. Thus $\psi(x) = c exp(\frac{-m\omega}{2\hbar}x^2)$ is a solution of the Schrodinger equation.

In order to find a general solution of the harmonic oscillator, eqn. (A.2) can be re-written to the following:

$$\frac{\partial^2 \psi(x)}{\partial x^2} + \left(\alpha - \beta^2 x^2\right)\psi(x) = 0 \tag{A.4}$$

with $\alpha = \frac{2mE}{\hbar^2}$ and $\beta = \frac{m\omega}{\hbar}$
a new variable is introduced: $z = \sqrt{\beta}x$, then eqn.(A.4) reads:

$$\frac{\partial^2 \psi(z)}{\partial z^2} + \left(\frac{\alpha}{\beta} - z^2\right)\psi(z) = 0 \tag{A.5}$$

In order to solve this new non-linear differential equation, let's assume the solution on the form: $\psi(z) = u(z)e^{\frac{-z^2}{2}}$. Again computing the 1st and 2nd derivatives of the wave function reads:

$$\frac{\partial \psi(z)}{\partial z} = (u' - uz)e^{\frac{-z^2}{2}}$$

$$\frac{\partial^2 \psi(z)}{\partial z^2} = (u'' - 2u'z - u + uz^2)e^{\frac{-z^2}{2}} \tag{A.6}$$

Inserting the expression of the 2nd derivative given by (A.6) back into eqn. (A.5), a new non-linear differential equation arises as a function of $u(z)$:

$$\frac{\partial^2 u(z)}{\partial z^2} - 2z\frac{\partial u}{\partial z} + \left(\frac{\alpha}{\beta} - 1\right)u(z) = 0 \tag{A.7}$$

Equation (A.7) has well known solutions for specific values of α and β when compared to the Hermite equation:

$$u''(z) - 2zu'(z) + 2nu(z) = 0, n \in \mathbb{N} \tag{A.8}$$

Thus the quantization arises from the restrictions on the nature of Hermite's equation:

$$\frac{\alpha}{\beta} = \frac{8\pi m E}{2\hbar\omega} = 2n + 1, n \in \mathbb{N}$$

The eigenvalues (i.e. eigenenergies) of H_{HO} are:

$$E = E_n = \hbar\omega(n + \frac{1}{2}), n \in \mathbb{N}$$

In order to solve the Hermite's equation (A.8), let's assume $u(z)$ on the form:

$$u(z) = H(z) = a_0 + a_1 z + a_2 z^2 + \cdots = \sum_{p=0}^{\infty} a_p z^p$$

Then computing the 1st and 2nd derivatives of $H(z)$ reads:

$$H'(z) = a_1 + 2a_2 z + 3a_3 z^2 + \cdots$$
$$= \sum_{p=0}^{\infty} p a_p z^{p-1}$$
$$H''(z) = 2a_2 + 3*2a_3 z + 4*3a_4 z^2 + \cdots$$
$$= \sum_{p=0}^{\infty} p(p+1) a_p z^{p-2}$$
$$= \sum_{p=0}^{\infty} (p+2)(p+1) a_{p+2} z^p$$

Back into eqn.(A.8), it gives the following relation between the coefficients:

$$a_{p+2} = \frac{-(2n - 2p)}{(p+1)(p+2)} a_p$$

Note that a_0 and a_1 are not obtained from the recursion, but from the differential equation itself.

The next step in the solution is to show that the series can be written in terms of $exp(-z^2)$ and that appropriate values can be assigned to the constants a_0 and a_1 to result in a well-behaved wave function. However the process to show it is rather tedious and can be found in advanced text books [58].

The Hermite polynomials $H_n(z)$ can be written as:

$$H_n(z) = (-1)^n e^{z^2} \frac{d^n}{dz^n}(e^{-z^2})$$

leading to the following first polynomials:

$$
\begin{array}{ll}
H_0(z) = & 1 \\
H_1(z) = & 2z \\
H_2(z) = & 2(2z-1) \\
H_3(z) = & 4(2z^3 - 3z) \\
\ldots
\end{array}
$$

Therefore, the eigenvectors of H_{HO} are:

$$\psi(z) = \psi_k(z) = N_k H_k(z) e^{\frac{-z^2}{2}}, k \in \mathbb{N}$$

with N_k a normalisation constant and $H_k(z)$ the Hermite polynomial.

As a summary, eigenvalues and eigenfunction of H_{HO} are given by

$$
\begin{cases}
E_n = & \hbar\omega(n + \frac{1}{2}) \\
\psi_n(z) = & N_n H_n(z) e^{\frac{-z^2}{2}}
\end{cases}
, n \in \mathbb{N} \quad , z = x\sqrt{\frac{m\omega}{\hbar}}
$$

A.1.2 N-Harmonic Oscillators with spin

A spinless particle of mass m in an isotropic harmonic potential has Hamiltonian:

$$H_{\mathrm{HO}} = -\frac{\hbar^2}{2m}\nabla^2 + \frac{1}{2}m\omega^2\|\vec{r}\|^2, \tag{A.9}$$

Scaling with proper energy and length units, i.e. $\hbar\omega$ $\sqrt{\hbar/m\omega}$ respectively [Simen Kvaal]. New hamiltonian

A.2 Single electron Quantum Dot (i.e. isotropic Quantum Harmonic Oscillator)

A.2.1 3D solution

A.2.2 2D solution

A.3 N-electrons Quantum Dots without e-e interactions = N particles HO

A.4 Exact solution of a 2-electrons Quantum Dots WITH e-e interactions (TAUT)

also detailed in a paper of Simen: "Harmonic oscillator eigenfunction expansions, quantum dots, and effective interactions" (august 2008)

Appendix B

Mathematical tools

B.1   The method of Lagrange Multipliers

In mathematical optimization, the method of Lagrange multipliers (named after Joseph Louis Lagrange) provides a strategy for finding the stationnary points of a function (and among them maxima/minima if the derivative of the function is defined for those points) subject to some constraints [59].

B.1.1   General approach of the method

For example (see figure B.1), consider the following optimization problem:

- maximize the **functional** $f(x, y)$

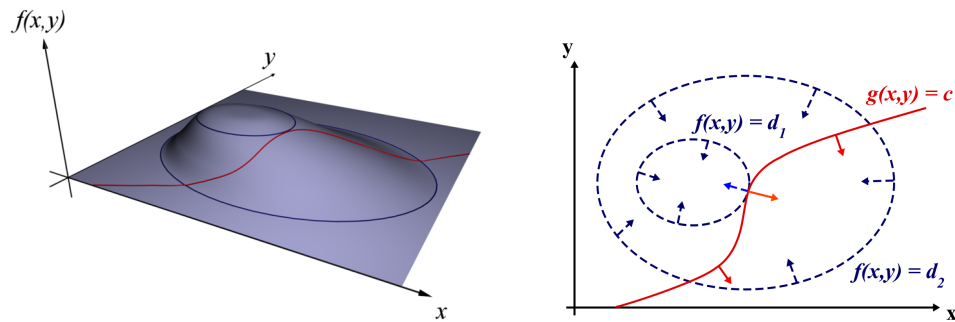- subject to the **constraint** $g(x, y) = c$

Figure B.1: Find x and y to maximize $f(x, y)$ subject to a constraint (shown in red) $g(x, y) = c$.
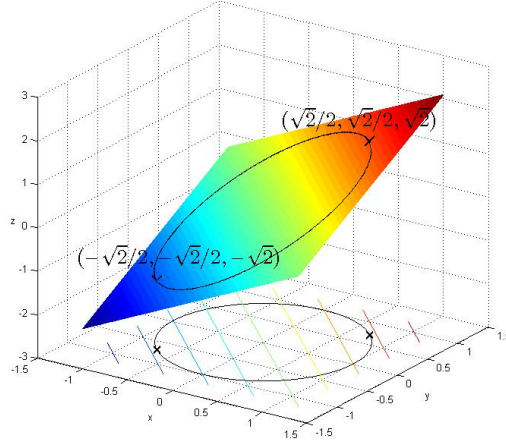
Figure B.2: Illustration of the constrained optimization problem.

We introduce a new variable (λ) called a Lagrange multiplier, and study the **Lagrange function** (or *Lagrangian*) defined by

$$\Lambda(x, y, \lambda) = f(x, y) - \lambda\,(g(x, y) - c) \tag{B.1}$$

If (x, y) is a maximum for the original constrained problem, then there exists a λ such that (x, y, λ) is a stationary point for the Lagrange function (stationary points are those points where the partial derivatives of Λ are zero). However, not all stationary points yield a solution of the original problem. Thus, the method of Lagrange multipliers yields a necessary condition for optimality in constrained problems.

B.1.2   Example

Let's use the method for a simple example:

Suppose you wish to maximize $f(x, y) = x + y$ subject to the constraint $x^2 + y^2 = 1$. The constraint is the unit circle as shown on figure B.2, and the level sets of f are diagonal lines (with slope -1), so one can see graphically that the maximum occurs at $(\sqrt{2}/2, \sqrt{2}/2)$ (and the minimum occurs at $(-\sqrt{2}/2, -\sqrt{2}/2)$)

Formally, we get from the constraint that $g(x, y) - c = x2 + y2 - 1$, and the Lagrange function reads

$$\Lambda(x, y, \lambda) = f(x, y) + \lambda(g(x, y) - c) = x + y + \lambda(x^2 + y^2 - 1) \tag{B.2}$$

Set the derivative $\partial\Lambda = 0$, which yields the system of equations:

$$\begin{cases} \dfrac{\partial\Lambda}{\partial x} = 1 + 2\lambda x = 0, & \text{(i)} \\[2mm] \dfrac{\partial\Lambda}{\partial y} = 1 + 2\lambda y = 0, & \text{(ii)} \\[2mm] \dfrac{\partial\Lambda}{\partial \lambda} = x^2 + y^2 - 1 = 0, & \text{(iii)} \end{cases} \qquad \text{(B.3)}$$

As always, the $\partial\lambda$ equation is the original constraint.

Combining the first two equations yields $x = y$ (explicitly, $\lambda \neq 0$, otherwise (i) yields $1 = 0$, so one has $x = -1/(2\lambda) = y$).

Substituting into (iii) yields $2x^2 = 1$, so $x = \pm\sqrt{2}/2$ and the stationary points are $(\sqrt{2}/2, \sqrt{2}/2)$ and $(-\sqrt{2}/2, -\sqrt{2}/2)$. Evaluating the objective function f on these yields $f(\sqrt{2}/2, \sqrt{2}/2) = \sqrt{2}$ and $f(-\sqrt{2}/2, -\sqrt{2}/2) = -\sqrt{2}$,

thus the maximum is $\sqrt{2}$, which is attained at $(\sqrt{2}/2, \sqrt{2}/2)$ and the minimum is $-\sqrt{2}$, which is attained at $(-\sqrt{2}/2, -\sqrt{2}/2)$.

Bibliography

[1] N.F. Johnson and M. Reina. The accuracy of the hartree-fock approximation for quantum dots. *Journal of Physics: Condensed Matter*, 4:623–628, September 1992.

[2] Daniela Pfannkuche, Vidar Gudmundsson, and Peter A. Maksym. Comparison of a hartree, a hartree-fock, and an exact treatment of quantum-dot helium. *Physical Review B*, 47(4):2244–2250, January 1993.

[3] Rune Albrigtsen. Computational environment for many-electron systems. Master's thesis, University of Oslo, March 2009.

[4] Simen Kvaal. *Analysis of many-body methods for quantum dots*. PhD thesis, University of Oslo, January 2009.

[5] Shubeur Rahman. Applications of quantum dots in the biological sciences. Simula Research Laboratory, Lysaker, Norway, January 2008.

[6] *Electron transport in quantum dots*, Proceedings of the Advanced Study Institute, 1997.

[7] Th. Heinzel. *Mesoscopic Electronics in Solid State Nanostructures*. Wiley-VCH, Weinheim, 2003.

[8] Kuppuswamy Kalyanasundaram. Cleavage of water by visible-light irradiation of colloidal cds solutions; inhibition of photocorrosion by ruo_2. *Angewandte Chemie International Edition in English*, 20(11):987–988, 2003.

[9] R. Rossetti, S. Nakahara, and L. E. Brus. Quantum size effects in the redox potentials, resonance raman spectra, and electronic spectra of cds crystallites in aqueous solution. *The Journal of Chemical Physics*, 79(2):1086–1088, 1983.

[10] C S Lent, P D Tougaw, W Porod, and G H Bernstein. Quantum cellular automata. *Nanotechnology*, 4(1):49–57, 1993.

[11] Marcel Bruchez, Mario Moronne, Peter Gin, Shimon Weiss, and Paul A. Alivisatos. Semiconductor nanocrystals as fluorescent biological labels. *Science*, 281(5385):2013–2016, September 1998.

[12] Warren C. W. Chan and Shuming Nie. Quantum dot bioconjugates for ultrasensitive nonisotopic detection. *Science*, 281(5385):2016–2018, September 1998.

[13] M. Baseer Haider, Jason L. Pitters, Gino A. DiLabio, Lucian Livadaru, Josh Y. Mutus, and Robert A. Wolkow. Controlled coupling and occupation of silicon atomic quantum dots at room temperature. *Physical Review Letters*, 102(4):046805, 2009.

[14] C. Weisbuch, H. Benisty, and R. Houdrï£¡. Overview of fundamentals and applications of electrons, excitons and photons in confined structures. *Journal of Luminescence*, 85(4):271 – 293, 2000.

[15] Igor L. Medintz, Tetsuo H. Uyeda, Ellen R. Goldman, and Hedi Mattoussi. Quantum dot bioconjugates for imaging, labelling and sensing. *Nat Mater*, 4(6):435–446, June 2005.

[16] Xiaohu Gao, Yuanyuan Cui, Richard M. Levenson, Leland W. Chung, and Shuming Nie. In vivo cancer targeting and imaging with semiconductor quantum dots. *Nat Biotech*, 22(8):969–976, 2004.

[17] Akiyoshi Hoshino, Ken ichi Hanaki, Kazuo Suzuki, and Kenji Yamamoto. Applications of t-lymphoma labeled with fluorescent quantum dots to cell tracing markers in mouse body. *Biochemical and Biophysical Research Communications*, 314(1):46 – 53, 2004.

[18] Evelyn B. Voura1, Jyoti K Jaiswal1, Hedi Mattoussi, and Sanford M. Simon. Tracking metastatic tumor cell extravasation with quantum dot nanocrystals and fluorescence emission-scanning microscopy. *Nature Medicine*, 10:993 – 998, 2004.

[19] Marijeta Kralj and Kresimir Pavelic. Medicine on a small scale. *EMBO reports*, 4(11):1008âĂŞ1012, 2003.

[20] Jessica O. Winter. *Development and optimization of quantum dot-neuron interfaces*. PhD thesis, The University of Texas at Austin, 2004.

[21] Hak Soo Choi, Wenhao Liu, Preeti Misra, Eiichi Tanaka, John P Zimmer, Binil Itty Ipe, Moungi G Bawendi, and John V Frangioni. Renal clearance of quantum dots. *Nat Biotech*, 25(10):1165–1170, October 2007.

[22] R. K. Willardson and Albert C. Beer. *Semiconductors and semimetals.* Academic Press, 1971.

[23] Walter A. Harrison. *Electronic Structure and the Properties of Solids: The Physics of the Chemical Bond.* Dover Publications, July 1989.

[24] H. Weller, H. M. Schmidt, U. Koch, and A. FojtikCorresponding. Photochemistry of colloidal semiconductors. onset of light absorption as a function of size of extremely small cds particles. *Chem. Phys. Lett.*, 124(6):557–560, 1986.

[25] Yigal Meir, Ned S. Wingreen, and Patrick A. Lee. Transport through a strongly interacting electron system: Theory of periodic conductance oscillations. *Phys. Rev. Lett.*, 66(23):3048–3051, Jun 1991.

[26] Stephanie M. Reimann and Matti Manninen. Electronic structure of quantum dots. *Rev. Mod. Phys.*, 74(1):1283–1342, November 2002.

[27] Hiroshi Mizuta, Heinz-Olaf Muller, Kazuhito Tsukagoshi, David Williams, Zahid Durrani, Andrew Irvine, Gareth Evans, Shuhei Amakawa, Kazuo Nakazato, and Haroon Ahmed. Nanoscale coulomb blockade memory and logic devices. *Nanotechnology*, 12(2):155–159, 2001.

[28] M. Ciorga, A. S. Sachrajda, P. Hawrylak, C. Gould, P. Zawadzki, S. Jullian, Y. Feng, and Z. Wasilewski. Addition spectrum of a lateral dot from coulomb and spin-blockade spectroscopy. *Phys. Rev. B*, 61(24):R16315–R16318, Jun 2000.

[29] N.F. Johnson and M.C. Payne. Exactly solvable model of interacting particles in a quantum dot. *Phys. Rev. Lett.*, 67:1157, 1991.

[30] D. Chaney and P. A. Maksym. Size-dependent suppression of spin relaxation in electrostatic quantum dots. *Physical Review B (Condensed Matter and Materials Physics)*, 75(3):035323, 2007.

[31] Stern F. Kumar A, Laux SE. Electron states in a gaas quantum dot in a magnetic field. *Physical Review B (Condensed Matter and Materials Physics)*, 42:5166–5175, Sept. 1990.

[32] M. Macucci, Karl Hess, and G. J. Iafrate. Electronic energy spectrum and the concept of capacitance in quantum dots. *Phys. Rev. B*, 48(23):17354–17363, Dec 1993.

[33] M. Macucci, Karl Hess, and G. J. Iafrate. Numerical simulation of shell-filling effects in circular quantum dots. *Phys. Rev. B*, 55(8):R4879–R4882, Feb 1997.

[34] M. Stopa. Quantum dot self-consistent electronic structure and the coulomb blockade. *Phys. Rev. B*, 54(19):13767–13783, Nov 1996.

[35] Walter Kohn. Cyclotron resonance and de haas-van alphen oscillations of an interacting electron gas. *Phys. Rev.*, 123(4):1242–1244, Aug 1961.

[36] Detlef Heitmann and Jörg P. Kotthaus. The spectroscopy of quantum dot arrays. *Physics Today*, 46(6):56–63, 1993.

[37] Detlef Heitmann. Far infrared spectroscopy of quantum-dots and antidot arrays. *Physica B: Condensed Matter*, 212(3):201 – 206, 1995. Proceedings of the Workshop on Novel Physics in Low-Dimensional Electron Systems.

[38] L. Brey, N. F. Johnson, and B. I. Halperin. Optical and magneto-optical absorption in parabolic quantum wells. *Phys. Rev. B*, 40(15):10647–10649, Nov 1989.

[39] F. M. Peeters. Magneto-optics in parabolic quantum dots. *Phys. Rev. B*, 42(2):1486–1487, Jul 1990.

[40] S. K. Yip. Magneto-optical absorption by electrons in the presence of parabolic confinement potentials. *Phys. Rev. B*, 43(2):1707–1718, Jan 1991.

[41] Q. P. Li, K. Karraï, S. K. Yip, S. Das Sarma, and H. D. Drew. Electrodynamic response of a harmonic atom in an external magnetic field. *Phys. Rev. B*, 43(6):5151–5154, Feb 1991.

[42] Ch. Sikorski and U. Merkt. Spectroscopy of electronic states in insb quantum dots. *Phys. Rev. Lett.*, 62(18):2164–2167, May 1989.

[43] Jed Dempsey, N. F. Johnson, L. Brey, and B. I. Halperin. Collective modes in quantum-dot arrays in magnetic fields. *Phys. Rev. B*, 42(18):11708–11713, Dec 1990.

[44] A Kwasniowski and J Adamowski. Effect of confinement potential shape on exchange interaction in coupled quantum dots. *Journal of Physics: Condensed Matter*, 20(21):215208 (8pp), 2008.

[45] Brian Harald Bransden and Charles Jean Joachain. *Physics of Atoms and Molecules; 2nd ed.* Prentice-Hall, Harlow, 2003.

[46] M. B. Tavernier, E. Anisimovas, F. M. Peeters, B. Szafran, J. Adamowski, and S. Bednarek. Four-electron quantum dot in a magnetic field. *Phys. Rev. B*, 68(20):205305, Nov 2003.

[47] Christopher J. Cramer. *Essentials of computational chemistry : theories and models.* John Wiley & Sons, 2008.

[48] Wikipedia. Ab initio quantum chemistry methods — Wikipedia, the free encyclopedia, 04 2009. [Online; accessed 9-April-2009].

[49] R. J. Bartlett. Many-body perturbation theory and coupled cluster theory for electron correlation in molecules. *Ann. Rev. Phys. Chem*, 32:359–401, 1981.

[50] Marcos Moshinsky and Yuri F. Smirnov. *The Harmonic Oscillator in Modern Physics: From Atoms to Quarks.* Taylor & Francis, 1996.

[51] Jos Thijssen. *Computational Physics.* Cambridge University Press, Cambridge, UK, 2007.

[52] O. Heinonen, E.K.U. Gross, and E. Runge. *Many-Particle Theory.* Hilger, 1991.

[53] Stanley Raimes. *Many-electron Theory.* North-Holland Publishing, 1972.

[54] Massimo Rontani. *Electronic States in Semiconductor Quantum Dots.* PhD thesis, Universita degli Studi di MODENA e REGGIO EMILIA, October 1999.

[55] E. Anisimovas and A. Matulis. Energy spectra of few-electron quantum dots. *J. Phys.: Condens. Matter*, 10(3):601–615, January 1998.

[56] S. M. Girvin and Terrence Jach. Interacting electrons in two-dimensional landau levels: Results for small clusters. *Phys. Rev. B*, 28(8):4506–4509, October 1983.

[57] E. Waltersson and E. Lindroth. Many-body perturbation theory calculations on circular quantum dots. *Phys. Rev. B*, 76(045314):045314, July 2007.

[58] J. E. House. *Fundamentals of Quantum Mechanics*. Academic Press, 1998.

[59] Wikipedia. Lagrange multipliers — Wikipedia, the free encyclopedia, 04 2009. [Online; accessed 13-April-2009].